

Quark contribution to the small- x evolution of color dipole

Ian Balitsky*

Physics Department, Old Dominion University, Norfolk Virginia 23529, USA
Theory Group, Jefferson Lab, 12000 Jefferson Avenue, Newport News, Virginia 23606, USA
 (Received 20 September 2006; published 2 January 2007)

The small- x deep inelastic scattering in the saturation region is governed by the nonlinear evolution of Wilson-lines operators. In the leading logarithmic approximation it is given by the Balitsky-Kovchegov (BK) equation for the evolution of color dipoles. In the next-to-leading order (NLO) the nonlinear equation gets contributions from quark and gluon loops. In this paper I calculate the quark-loop contribution to small- x evolution of Wilson lines in the NLO. It turns out that there are no new operators at the one-loop level—just as at the tree level, the high-energy scattering can be described in terms of Wilson lines. In addition, from the analysis of quark loops I find that the argument of coupling constant in the BK equation is determined by the size of the parent dipole rather than by the size of produced dipoles. These results are to be supported by future calculation of gluon loops.

DOI: [10.1103/PhysRevD.75.014001](https://doi.org/10.1103/PhysRevD.75.014001)

PACS numbers: 12.38.Bx, 11.15.Kc, 12.38.Cy

I. INTRODUCTION

At high energies the particles move very fast along straight lines, hence they can be described by Wilson lines $U^\eta(x_\perp)$ —gauge factors ordered along straight-line classical trajectory of the particle moving with rapidity η at the transverse impact parameter x_\perp (for a review, see Ref. [1]). For deep inelastic scattering, the propagation of a quark-antiquark pair moving along straight lines and separated by a distance in the transverse direction can be approximated by the color dipole $U(x_\perp)U^\dagger(y_\perp)$ —two Wilson lines ordered along the direction collinear to quarks' velocity. The structure function of a hadron is then proportional to a matrix element of the color dipole operator

$$\mathcal{U}^\eta(x_\perp, y_\perp) = 1 - \frac{1}{N_c} \text{Tr}\{U^\eta(x_\perp)U^{\dagger\eta}(y_\perp)\}, \quad (1)$$

switched between the target's states ($N_c = 3$ for QCD). Approximately, the gluon parton density is

$$x_B G(x_B, \mu^2 = Q^2) \simeq \langle p | \mathcal{U}^\eta(x_\perp, 0) | p \rangle |_{x_\perp^2 = Q^{-2}}, \quad (2)$$

where $\eta = \ln \frac{1}{x_B}$ and $x_B = \frac{Q^2}{2(p \cdot q)}$ is the Bjorken variable.

The small- x behavior of the structure functions is governed by the small- x evolution of color dipoles [2,3]. For sufficiently small dipoles $x_\perp^2 \sim Q^{-2}$ so $\alpha_s(Q) \ll 1$ and we can use pQCD. At high (but not asymptotic) energies we can use the leading logarithmic approximation (LLA) where $\alpha_s \ll 1$, $\alpha_s \ln x_B \sim 1$. In the LLA, the high-energy amplitudes in pQCD are described by the BFKL equation [4] leading to the power behavior $F_2(x_B) \sim x_B^{-12(\alpha_s/\pi) \ln 2}$. However, the example of DIS from very large nuclei shows that the BFKL equation is not sufficient to describe the small- x behavior of structure functions even in the LLA. Indeed, at sufficiently large atomic number A we get an additional parameter $\alpha_s A^{1/6} \sim 1$ which must be taken into

account exactly to all orders of the expansion in this parameter. The situation is essentially semiclassical: we have $\alpha_s \ll 1$ and $\alpha_s F_{\mu\nu}/m^2 \sim 1$ where $F_{\mu\nu}$ is the strong field of the nucleus gluon cloud and m^2 is the characteristic momentum scale. Thus we need the LLA in the semiclassical QCD (sQCD): $\alpha_s \ll 1$, $\alpha_s \ln x_B \sim 1$, $\alpha_s F_{\mu\nu}/m^2 \sim 1$. This situation appears to be general for sufficiently low x_B : even for the proton, where we do not have the large parameter A to start with, the power behavior of gluon parton density will lead to the huge number of partons in the target leading to the state of saturation [5] described by color glass condensate in sQCD [6,7].

The LLA evolution equation for the color dipoles is nonlinear [8,9]:

$$\begin{aligned} \frac{d}{d\eta} \mathcal{U}(x, y) = & \frac{\alpha_s N_c}{2\pi^2} \int d^2z \frac{(x-y)^2}{(x-z)^2(z-y)^2} [\mathcal{U}(x, z) \\ & + \mathcal{U}(y, z) - \mathcal{U}(x, y) - \mathcal{U}(x, z)\mathcal{U}(z, y)]. \end{aligned} \quad (3)$$

The first three terms correspond to the linear BFKL evolution and describe the parton emission while the last term is responsible for the parton annihilation. For sufficiently high x_B the parton emission balances the parton annihilation so the partons reach the state of saturation with the characteristic transverse momentum Q_s growing with x_B as $e^{c \ln x_B}$. The argument of the coupling constant in Eq. (3) is left undetermined in the LLA, and usually it is set by hand to be Q_s . Careful analysis of this argument is very important from both theoretical and experimental points of view. From the theoretical viewpoint, we need to know whether the coupling constant is determined by the size of the original dipole $|x-y|$ or of the size of the produced dipoles $|x-z|$ and/or $|z-y|$ since we may get a very different behavior of the solutions of Eq. (3) (although first numerical simulations indicate a slow dependence of the cross section on the choice of the scale [10]). On the

*Electronic address: balitsky@jlab.org

experimental side, the cross section is proportional to some power of the coupling constant so the argument determines how big (or how small) is the cross section. The typical argument of α_s is the characteristic transverse momenta of the process. For high enough energies, they are believed to be of order of the saturation scale Q_s which is $\sim 2 \div 3$ GeV for the LHC collider. Thus, we see that even the difference

between $\alpha(Q_s)$ and $\alpha(2Q_s)$ can make a huge impact on the cross section.

The argument of the coupling constant cannot be determined in the LLA so the next-to-leading order (NLO) calculation is in order. In the next-to-leading order the nonlinear Eq. (3) looks as follows ($x, y, z \dots$ are the transverse coordinates)

$$\begin{aligned} \frac{d}{d\eta} \text{Tr}\{U_x U_y^\dagger\} &= \frac{1}{2\pi^2} \int d^2z \left(\alpha_s \frac{(x-y)^2}{(x-z)^2(z-y)^2} + \alpha_s^2 K_{\text{NLO}}(x, y, z) \right) [\text{Tr}\{U_x U_z^\dagger\} \text{Tr}\{U_z U_y^\dagger\} - N_c \text{Tr}\{U_x U_y^\dagger\}] \\ &+ \alpha_s^2 \int d^2z d^2z' (K_4(x, y, z, z') \{U_x, U_{z'}, U_z, U_y^\dagger\} + K_6(x, y, z, z') \{U_x, U_{z'}, U_z, U_z, U_z^\dagger, U_y^\dagger\}), \end{aligned} \quad (4)$$

where K_{NLO} is the next-to-leading-order correction to the dipole kernel and K_4 and K_6 are the coefficients in front of the (tree) four- and six-Wilson-line operators with arbitrary white arrangements of color indices. Note that K_{NLO} must describe the nonforward NLO BFKL contribution found recently in Ref. [11]. (The contribution $\sim K_6$ proportional to six Wilson-line operators the was obtained in Ref. [12]). The calculation of the quark part of the kernel is performed in the present paper and the last remaining part of Eq. (4)—the calculation of the gluon part of K_{NLO} and K_4 —is in progress.

It should be mentioned that NLO result does not lead automatically to the argument of coupling constant in front of the leading term in Eq. (4). In order to get this argument, we can use the renormalon-based approach [13]: first we get the quark part of the running coupling constant coming from the bubble chain of quark loops and then make a conjecture that the gluon part of the β -function will follow that pattern (see the discussion in Refs. [14,15]).

As we demonstrate below, the result is that the value of coupling constant is determined by the size of the original dipole rather than the size of the produced dipoles:

$$\begin{aligned} \frac{d}{d\eta} \mathcal{U}(x, y) &= \frac{\alpha_s((x-y)^2) N_c}{2\pi^2} \int d^2z \frac{(x-y)^2}{(x-z)^2(z-y)^2} \\ &\times [\mathcal{U}(x, z) + \mathcal{U}(y, z) - \mathcal{U}(x, y) \\ &- \mathcal{U}(x, z)\mathcal{U}(z, y)] + \dots \end{aligned} \quad (5)$$

(Actually, following the BLM procedure [14], it is more natural to choose argument of α_s as $(x-y)_\perp^2 e^{5/3}$, see the discussion in Sec. IV).

The paper is organized as follows. In Sec. II I recall the derivation of the Balitsky-Kovchegov (BK) equation in the leading order in α_s . In Sec. III, which is central to the paper, I calculate the quark contribution to the small- x evolution kernel of Wilson-line operators. In Sec. IV I present the arguments that the coupling constant in the BK equation is determined by the size $(x-y)_\perp$ of the

parent dipole. The light-cone expansion of the quark-loop propagator is performed in the Appendix A. Appendix B is devoted to the comparison of our result with the interpretation of the NLO BK equation in terms of three coupling constants suggested in the recent preprint [16].

II. DERIVATION OF THE BK EQUATION

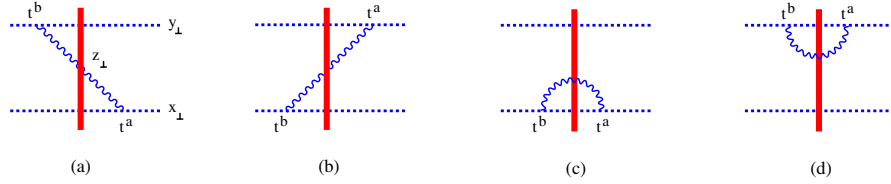
Before discussion of the small- x evolution of color dipole in the next-to-leading approximation it is instructive to recall the derivation of the leading-order (BK) evolution equation. As discussed in the Introduction, the dependence of the structure functions on x_B comes from the dependence of Wilson-line operators

$$\begin{aligned} U^\eta(x_\perp) &= \text{P exp} \left\{ ig \int_{-\infty}^{\infty} du p_\mu^\eta A^\mu(u p^\eta + x_\perp) \right\}, \\ p^\eta &\equiv p_1 + e^{-\eta} p_2 \end{aligned} \quad (6)$$

on the slope of the supporting line. Here p_1 and p_2 are the lightlike vectors such that $q = p_1 - x_B p_2$ and $p = p_2 + \frac{m^2}{s} p_1$ where p is the momentum of the target and m is the mass. Throughout the paper, we use the Sudakov variables $p = \alpha p_1 + \beta p_2 + p_\perp$ and the notations $x_\bullet \equiv x_\mu p_1^\mu$ and $x_* \equiv x_\mu p_2^\mu$ related to the light-cone coordinates: $x_* = x^+ \sqrt{s/2}$, $x_\bullet = x^- \sqrt{s/2}$.

To find the evolution of the color dipole (1) with respect to the slope of the Wilson lines in the leading log approximation, we consider the matrix element of the color dipole between (arbitrary) target states and integrate over the gluons with rapidities $\eta_1 > \eta > \eta_2 = \eta_1 - \Delta\eta$ leaving the gluons with $\eta < \eta_2$ as the background field (to be integrated over later). In the frame of gluons with $\eta \sim \eta_1$ the fields with $\eta < \eta_2$ shrink to a pancake and we obtain the four diagrams shown in Fig. 1

The (background-Feynman) gluon propagator in a shock-wave external field has the form [9,17]


 FIG. 1 (color online). Leading-order diagrams for the small- x evolution of color dipole.

$$\begin{aligned}
 \langle A_\mu^a(x) A_\nu^b(y) \rangle &= \theta(x_* y_*) \left(x \left| \frac{g_{\mu\nu} \delta^{ab}}{i(p^2 + i\epsilon)} \right| y \right) - \theta(x_*) \theta(-y_*) \int_0^\infty d\alpha \frac{e^{-i\alpha(x-y)_\bullet}}{4\alpha^2} \left(x_\perp \left| e^{-i(p_\perp^2/\alpha s)x_*} \left[2\alpha g_{\mu\nu} U \right. \right. \right. \\
 &+ \frac{4}{s} (i\partial_\mu p_{2\nu} U - p_{2\mu} i\partial_\nu U) - \frac{4p_{2\mu} p_{2\nu}}{\alpha s^2} \partial_\perp^2 U \left. \left. \left. \right| y_\perp \right)^{ab} - \theta(-x_*) \theta(y_*) \int_0^\infty d\alpha \frac{e^{i\alpha(x-y)_\bullet}}{4\alpha^2} \right. \\
 &\times \left. \left. \left. \left(x_\perp \left| e^{-i(p_\perp^2/\alpha s)x_*} \left[2\alpha g_{\mu\nu} U^\dagger - \frac{4}{s} (i\partial_\mu U^\dagger p_{2\nu} - p_{2\mu} i\partial_\nu U^\dagger) - \frac{4p_{2\mu} p_{2\nu}}{\alpha s^2} \partial_\perp^2 U^\dagger \right] e^{i(p_\perp^2/\alpha s)y_*} \right| y_\perp \right)^{ab} \right) \right) \quad (7)
 \end{aligned}$$

where $\partial_\perp^2 \equiv -\partial_i \partial^i$. Hereafter use Schwinger's notations $(x|F(p)|y) \equiv \int \tilde{d}p F(p) e^{-ip \cdot (x-y)}$ and $(x_\perp|F(p_\perp)|y) \equiv \int \tilde{d}p e^{i(p \cdot x - y)_\perp}$ (the scalar product of the four-dimensional vectors in our notations is $x \cdot y = \frac{z}{s}(x_* y_\bullet + x_\bullet y_*) - (x, y)_\perp$). We obtain

$$\begin{aligned}
 \left\{ \int_0^\infty du \int_{-\infty}^0 dv A_\bullet^a(u p^{\eta_1} + x_\perp) A_\bullet^b(v p^{\eta_1} + y_\perp) \right\}_{\text{Fig.1a}} &= -2\alpha_s \int_{e^{-\eta_2}}^\infty \frac{d\alpha}{\alpha} \left(x_\perp \left| \frac{1}{p_\perp^2 + \alpha^2 e^{-2\eta_1 s}} \partial_\perp^2 U^{ab} \right. \right. \\
 &\times \left. \left. \frac{1}{p_\perp^2 + \alpha^2 e^{-2\eta_1 s}} \right| y_\perp \right). \quad (8)
 \end{aligned}$$

Formally, the integral over α diverges at the lower limit, but since we integrate over the rapidities $\eta > \eta_2$ we get in the LLA

$$\begin{aligned}
 \left\{ \int_0^\infty du \int_{-\infty}^0 dv A_\bullet^a(u p_\eta + x_\perp) A_\bullet^b(v p_\eta + y_\perp) \right\}_{\text{Fig.1a}} &= -2\alpha_s \Delta\eta \left(x_\perp \left| \frac{1}{p_\perp^2} \partial_\perp^2 U^{ab} \frac{1}{p_\perp^2} \right. \right. \\
 &= -2\alpha_s \Delta\eta \int d^2 z_\perp \left(x_\perp \left| \frac{p_i}{p_\perp^2} \right. \right. \\
 &\times \left. \left. (2U_z - U_x - U_y)^{ab} \left(z_\perp \left| \frac{p_i}{p_\perp^2} \right. \right| y_\perp \right) \right) \quad (9)
 \end{aligned}$$

and therefore

$$\{U_x \otimes U_y^\dagger\}_{\text{Fig.1a}}^{\eta_1} = -\frac{\alpha_s}{2\pi^2} \Delta\eta \{t^a U_x \otimes t^b U_y^\dagger\}_{\eta_2} \int d^2 z_\perp \frac{(x-z, y-z)_\perp}{(x-z)_\perp^2 (y-z)_\perp^2} (2U_z^{\eta_2} - U_x^{\eta_2} - U_y^{\eta_2})^{ab}. \quad (10)$$

The contribution of the diagram in Fig. 1(b) is obtained from Eq. (10) by the replacement $t^a U_x \otimes t^b U_y^\dagger \rightarrow U_x t^b \otimes U_y^\dagger t^a$, $x \leftrightarrow y$ and the two remaining diagrams are obtained from Eq. (9) by taking $y = x$ [Fig. 1(c)] and $x = y$ [Fig. 1(d)]. Finally, one obtains

$$\begin{aligned}
 \{U_x \otimes U_y^\dagger\}_{\text{Fig.1}}^{\eta_1} &= -\frac{\alpha_s \Delta\eta}{2\pi^2} \{t^a U_x \otimes t^b U_y^\dagger + U_x t^b \otimes U_y^\dagger t^a\}_{\eta_2} \int d^2 z_\perp \frac{(x-z, y-z)_\perp}{(x-z)_\perp^2 (y-z)_\perp^2} (2U_z^{\eta_2} - U_x^{\eta_2} - U_y^{\eta_2})^{ab} + \frac{\alpha_s \Delta\eta}{\pi^2} \\
 &\times \{t^a U_x t^b \otimes U_y^\dagger\}_{\eta_2} \int \frac{d^2 z_\perp}{(x-z)_\perp^2} (U_z^{\eta_2} - U_x^{\eta_2})^{ab} + \frac{\alpha_s \Delta\eta}{\pi^2} \{U_x \otimes t^b U_y^\dagger t^a\}_{\eta_2} \int \frac{d^2 z_\perp}{(y-z)_\perp^2} (U_z^{\eta_2} - U_y^{\eta_2})^{ab}. \quad (11)
 \end{aligned}$$

For the color dipole (1) one easily gets the BK Eq. (3).

III. QUARK CONTRIBUTION TO THE NLO BK KERNEL

A. Quark loop in the momentum representation

There are two types of quark contribution in the NLO: with quarks in the loop interacting with the shock wave

[see Fig. 2(a)] or without [Fig. 2(b)]. (In principle, there could have been the contribution coming from the quark loop which lies entirely in the shock wave, but we will demonstrate below that it vanishes).

The quark propagator in a shock-wave background has the form [9]:

$$\begin{aligned} \psi(x)\bar{\psi}(y) = & \theta(x_*y_*) \left(x \left| \frac{i\not{p}}{p^2 + i\epsilon} \right| y \right) + \theta(x_*)\theta(-y_*) \int_0^\infty \frac{d\alpha}{2\alpha^2 s} e^{-i\alpha(x-y)_\perp \cdot (x_\perp | (\alpha\hat{p}_1 + \hat{p}_\perp) e^{-i(p_\perp^2/\alpha s)x_*} \hat{p}_2 U e^{i(p_\perp^2/\alpha s)y_*} (\alpha\hat{p}_1 \\ & + \hat{p}_\perp) | y_\perp) - \theta(-x_*)\theta(y_*) \int_{-\infty}^0 \frac{d\alpha}{2\alpha^2 s} e^{-i\alpha(x-y)_\perp \cdot (x_\perp | (\alpha\hat{p}_1 + \hat{p}_\perp) e^{-i(p_\perp^2/\alpha s)x_*} \hat{p}_2 U^\dagger e^{i(p_\perp^2/\alpha s)y_*} (\alpha\hat{p}_1 + \hat{p}_\perp) | y_\perp) \end{aligned} \quad (12)$$

Multiplying two propagators one gets at $x'_* > 0, y'_* < 0$

$$\begin{aligned} \bar{\psi}(x')t^a\not{p}_1\psi(x')\bar{\psi}(y')t^b\not{p}_1\psi(y') = & \int_0^\infty \frac{d\alpha}{16\pi\alpha^3} \int_0^1 \frac{dv}{\bar{v}^2 v^2} e^{-i\alpha(x'-y')_\perp \cdot \text{tr Tr}(x'_\perp | \not{p}_\perp e^{-i(p_\perp^2/\alpha v s)x'_*} U e^{i(p_\perp^2/\alpha v s)y'_*} \not{p}_\perp | y'_\perp) \\ & \times t^b(y'_\perp | \not{p}_\perp e^{i(p_\perp^2/\alpha v s)y'_*} U^\dagger e^{i(p_\perp^2/\alpha v s)x'_*} \not{p}_\perp | x'_\perp), \end{aligned} \quad (13)$$

where tr stands for the trace over spinor indices and v is the part of the gluon's longitudinal momentum α carried by the quark (hereafter we use the notation $\bar{v} = 1 - v$). The quark-loop contribution to the gluon propagator is

$$\langle A_\bullet^a(x)A_\bullet^b(y) \rangle = \int d^4x d^4y' d^4q d^4q' \frac{e^{-iq(x-x')}}{q^2 + i\epsilon} \frac{e^{-iq'(y'-y)}}{q'^2 + i\epsilon} \langle \bar{\psi}(x')t^a\not{p}_1\psi(x')\bar{\psi}(y')t^b\not{p}_1\psi(y') \rangle.$$

Performing the integration over the coordinates of quark-quark-gluon vertices x' and y' one obtains

$$\begin{aligned} \langle A_\bullet^a(x)A_\bullet^b(y) \rangle = & 2\alpha_s^2 n_f \int d^2z d^2z' \int d^2k_1 d^2k'_1 d^2k_2 d^2k'_2 e^{i(k_1, x-z)_\perp + i(k'_1, x-z')_\perp - i(k_2, y-z)_\perp - i(k'_2, y-z')_\perp} \int_0^\infty \frac{d\alpha}{\alpha^3} \text{Tr}\{t^a U_z t^b U_{z'}^\dagger\} \\ & \times \int_0^1 dv \frac{(k_1, k_2)(k'_1, k'_2) + (k_1, k'_1)(k_2, k'_2) - (k_1, k'_2)(k'_1, k_2)}{[(k_1 + k'_1)^2 \bar{v}v - k_1^2 \bar{v} - k_1'^2 v][(k_2 + k'_2)^2 \bar{v}v - k_2^2 \bar{v} - k_2'^2 v]} \\ & \times [e^{-i[(k_1 + k'_1)_\perp^2/\alpha s]x_*} - e^{-i[(k_1^2/v) + (k_1'^2/\bar{v})](x_*/\alpha s)}][e^{-i[(k_2 + k'_2)_\perp^2/\alpha s]y_*} - e^{-i[(k_2^2/v) + (k_2'^2/\bar{v})](y_*/\alpha s)}] \end{aligned} \quad (14)$$

so the contribution of the diagram in Fig. 2(a) takes the form

$$\begin{aligned} \left\{ \int_0^\infty du \int_{-\infty}^0 dv A_\bullet^a(up_1 + x_\perp) A_\bullet^b(vp_1 + y_\perp) \right\}_{\text{Fig.2a}} = & -8\alpha_s^2 n_f \int_0^\infty \frac{d\alpha}{\alpha} \int dz dz' \int d^2k_1 d^2k'_1 d^2k_2 d^2k'_2 \\ & \times e^{i(k_1, x-z)_\perp + i(k'_1, x-z')_\perp - i(k_2, y-z)_\perp - i(k'_2, y-z')_\perp} \text{Tr}\{t^a U_z t^b U_{z'}^\dagger\} \\ & \times \int_0^1 dv \frac{(k_1, k_2)(k'_1, k'_2) + (k_1, k'_1)(k_2, k'_2) - (k_1, k'_2)(k'_1, k_2)}{(k_1 + k'_1)^2 (k_2 + k'_2)^2 (k_1^2 v + k_1'^2 \bar{v})(k_2^2 v + k_2'^2 \bar{v})}, \end{aligned} \quad (15)$$

where n_f is a number of light quarks ($n_f = 3$ for the momenta $Q_s \sim 1 \div 2$ GeV) and Tr stands for the trace over color indices. The variable v is the fraction of the gluon's momentum α carried by the quark.

To calculate this diagram we use the dimensional regularization and change the dimension of the transverse space to $d = 2 - 2\epsilon$. The calculation yields

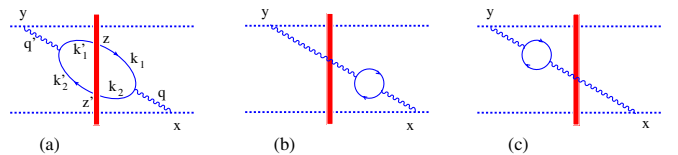


FIG. 2 (color online). First set of diagrams for the quark-loop contribution to the evolution of the color dipole.

$$\begin{aligned}
 \text{Tr}\{U_x U_y^\dagger\}_{\text{Fig.2a}} &= -\frac{4\alpha_s^2}{\pi} n_f \Delta \eta \text{Tr}\{t^a U_x t^b U_y^\dagger\} \int \tilde{d}^d p \tilde{d}^d q \tilde{d}^d q' \frac{e^{i(p,x)_\perp - i(p-q-q',y)_\perp}}{p^2(p-q-q')^2} \int_0^1 dv du \left[-(q+q')^2 \frac{\bar{u}u\Gamma(\epsilon)\mu^{2\epsilon}}{(P^2\bar{v}v + Q^2\bar{u}u)^\epsilon} \right. \\
 &+ \frac{\Gamma(1+\epsilon)\mu^{2\epsilon}}{(P^2\bar{v}v + Q^2\bar{u}u)^{1+\epsilon}} \{P^2[\bar{v}v(q,q') - \bar{u}uQ^2 + 2\bar{u}u\bar{v}v(q^2 + q'^2)] - 2\bar{u}u\bar{v}v(P,q)(P,q') + \bar{u}u(1-2u) \\
 &\times [\bar{v}v(q,q')(P,q+q') + \bar{v}q^2(P,q') + vq'^2(P,q)] + \bar{u}^2u^2Q^2(q+q')^2\} \left. \right] \text{Tr}\{t^a U(q)t^b U^\dagger(q')\}, \quad (16)
 \end{aligned}$$

where $P \equiv p - (q + q')u$, $Q^2 = q_\perp^2 \bar{v} + q'^2 v$ and we use the notation $\int \tilde{d}^d p_\perp \equiv \int \frac{d^d p_\perp}{(2\pi)^d}$.

The contribution of two diagrams in Fig. 2(b) and 2(c) is

$$\begin{aligned}
 &2n_f \alpha_s^2 \Delta \eta \text{tr}\{t^a U_x t^b U_y^\dagger\} \frac{\mu^{2\epsilon}}{\pi} B(2-\epsilon, 2-\epsilon) \\
 &\times \left(x_\perp \left| \frac{1}{p_\perp^2} \left\{ \frac{\Gamma(\epsilon)}{(p_\perp^2)^\epsilon}, \partial_\perp^2 U^{ab} \right\} \frac{1}{p_\perp^2} \right| y_\perp \right), \quad (17)
 \end{aligned}$$

where $B(a, b) = \Gamma(a)\Gamma(b)/\Gamma(a+b)$. The contribution of diagrams in Fig. 3 is obtained from the sum of Eq. (16) and (17) by the $x \leftrightarrow y$ replacement in the coefficient in front of $\text{tr}\{t^a U_x t^b U_y^\dagger\}$ and the contribution of the diagram in Fig. 4 by taking $y \rightarrow x$ in this coefficient and changing the sign. Similarly, the diagram in Fig. 5 is obtained by taking $x \rightarrow y$. The sum of all diagrams has the form

$$\begin{aligned}
 \text{Tr}\{U_x U_y^\dagger\} &= -\frac{\alpha_s^2}{\pi} n_f \Delta \eta \text{Tr}\{t^a U_x t^b U_y^\dagger\} \left(\int \frac{\tilde{d}^d p \tilde{d}^d q \tilde{d}^d q'}{p^2(p-q-q')^2} (e^{i(p,x)_\perp} - e^{i(p,y)_\perp})(e^{-i(p-q-q',x)_\perp} - e^{-i(p-q-q',y)_\perp}) \right. \\
 &\times \int_0^1 dudv \left[(q+q')^2 \frac{4\bar{u}u\Gamma(\epsilon)\mu^{2\epsilon}}{(P^2\bar{v}v + Q^2\bar{u}u)^\epsilon} - 4 \frac{\Gamma(1+\epsilon)\mu^{2-d}}{(P^2\bar{v}v + Q^2\bar{u}u)^{1+\epsilon}} \{P^2[\bar{v}v(q,q') - \bar{u}uQ^2 + 2\bar{u}u\bar{v}v(q^2 + q'^2)] \right. \\
 &- 2\bar{u}u\bar{v}v(P,q)(P,q') + \bar{u}u(1-2u)[\bar{v}v(q,q')(P,q+q') + \bar{v}q^2(P,q') + vq'^2(P,q)] + \bar{u}^2u^2Q^2(q+q')^2\} \left. \right] \\
 &\times \text{Tr}\{t^a U(q_\perp)t^b U^\dagger(q'_\perp)\} - 2\mu^{2\epsilon} B(2-\epsilon, 2-\epsilon) \left[2 \left(x_\perp \left| \frac{1}{p_\perp^2} \left\{ \frac{\Gamma(\epsilon)}{p_\perp^{2\epsilon}}, \partial_\perp^2 U^{ab} \right\} \frac{1}{p_\perp^2} \right| y_\perp \right) \right. \\
 &- \left. \left(x_\perp \left| \frac{1}{p_\perp^2} \left\{ \frac{\Gamma(\epsilon)}{p_\perp^{2\epsilon}}, \partial_\perp^2 U^{ab} \right\} \frac{1}{p_\perp^2} \right| x_\perp \right) - \left(y_\perp \left| \frac{1}{p_\perp^2} \left\{ \frac{\Gamma(\epsilon)}{p_\perp^{2\epsilon}}, \partial_\perp^2 U^{ab} \right\} \frac{1}{p_\perp^2} \right| y_\perp \right) \right] \\
 &+ \frac{1}{3\epsilon} \left[2 \left(x_\perp \left| \frac{1}{p_\perp^2} \partial_\perp^2 U^{ab} \frac{1}{p_\perp^2} \right| y_\perp \right) - \left(x_\perp \left| \frac{1}{p_\perp^2} \partial_\perp^2 U^{ab} \frac{1}{p_\perp^2} \right| x_\perp \right) - \left(y_\perp \left| \frac{1}{p_\perp^2} \partial_\perp^2 U^{ab} \frac{1}{p_\perp^2} \right| y_\perp \right) \right] \quad (18)
 \end{aligned}$$

where the last term $\sim \frac{1}{3\epsilon}$ is a counterterm calculated in the Appendix A.

B. Quark-loop inside the shock wave

Let us consider the diagram in Fig. 6 with the quark loop inside the shock wave of width $\lambda = \Delta z_* \sim \frac{s}{m^2} e^{-\eta_2}$ where m^2 is some characteristic mass scale of order of Q^2 . From the form of the perturbative propagator

$$\begin{aligned}
 \left(z \left| \frac{1}{p^2 + i\epsilon} \right| z' \right) &= \frac{s}{8\pi x_*} \int_0^\infty \frac{d\alpha}{\alpha} \\
 &\times e^{-i\alpha(z-z') \cdot -i[(z-z')_\perp^2 / (4(z-z')_*)] \alpha s},
 \end{aligned}$$

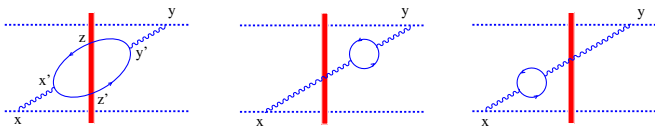


FIG. 3 (color online). Second set of diagrams for the quark-loop contribution.

we see that the characteristic transverse scale inside the shock wave is

$$(z - z')_\perp^2 \sim \frac{\lambda}{\alpha s} \simeq m^{-2} \frac{e^{-\eta_2}}{\alpha} \ll m^{-2}, \quad (19)$$

and therefore the contribution of the diagram in Fig. 6 reduces to the contribution of some operator *local* in the transverse space. By dimensional arguments, this local operator must have the same twist as the operator describing the interaction of the gluon with the shock wave at the tree level. In the leading order in α_s , the vertex of interaction of gluon with the shock-wave field is proportional to

$$\partial_\perp^2 U = -ig[DG] + 2g^2[GG], \quad (20)$$

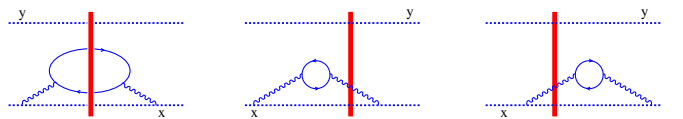


FIG. 4 (color online). Third set of diagrams for the quark-loop contribution.

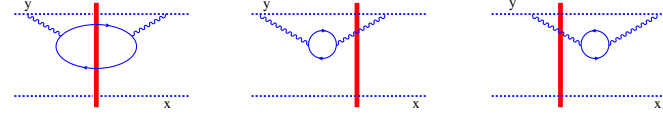


FIG. 5 (color online). Fourth set of diagrams for the quark-loop contribution.

where

$$\begin{aligned}
 [DG] &\equiv \int du [\infty p_1, up_1]_x D^i G_{i\bullet}(up_1 + x_\perp) \\
 &\quad \times [up_1, -\infty p_1]_x, \\
 [GG] &\equiv \int dudv \theta(u-v) [\infty p_1, up_1]_x G_{\bullet i}(up_1 + x_\perp) \\
 &\quad \times [up_1, vp_1]_x G^i_{\bullet}(vp_1 + x_\perp) [vp_1, -\infty p_1]_x. \quad (21)
 \end{aligned}$$

These operators have twist 2 so a possible local operator describing the gluon interaction with the shock wave at the one-loop level must also be of twist 2. To find this local

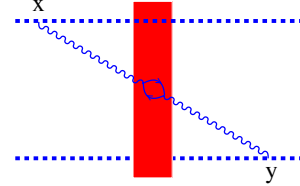


FIG. 6 (color online). Quark loop inside the shock wave.

operator, we consider (the quark-loop contribution to) the color dipole $\text{tr}\{U_x U_y^\dagger\}$ at small $(x-y)_\perp^2 \rightarrow 0$ and compare the expansion of the contribution of the diagrams in Fig. 2 to the exact calculation of the light-cone expansion of $\text{tr}\{U_x U_y^\dagger\}$ in QCD (up to twist-2 level), see Fig. 7.

The first step is the light-cone expansion of the sum of the diagrams in the in Figs. 2–5 in the shock-wave background. The light-cone expansion of Eq. (18) at $x_\perp \rightarrow y_\perp$ starts with terms quadratic in q' . They lead to the operators $\partial^2 U_x$ and $\partial_i U_x \partial_i U_x^\dagger$ (in the leading order we do not distinguish between U_x and U_y):

$$\begin{aligned}
 \text{Tr}\{\partial_i U_x \partial_i U_y^\dagger\}^{x \rightarrow y_\perp} &\stackrel{\alpha_s^2}{\pi} n_f \Delta \eta U_x^{ab} \left[\frac{4}{3} \mu^{2-d} B(1-\epsilon, 1-\epsilon) \left(x_\perp \left| \left(\left[3 - \frac{1}{\epsilon} \right] \delta_{ij} - \frac{p_i p_j}{p_\perp^2} \right) \frac{\Gamma(1+\epsilon)}{(p_\perp^2)^{1+\epsilon}} \right| y_\perp \right) \text{Tr}\{t^a \partial_i U_x t^b \partial_j U_x^\dagger\} \right. \\
 &\quad \left. + 4 \mu^{2-d} B(2-\epsilon, 2-\epsilon) \left(x_\perp \left| \frac{\Gamma(\epsilon)}{(p_\perp^2)^{1+\epsilon}} \right| y_\perp \right) \partial_\perp^2 U_x^{ab} - \frac{1}{3\epsilon} \left(x_\perp \left| \frac{1}{p_\perp^2} \right| y_\perp \right) \partial_\perp^2 U_x^{ab} \right] \\
 &= \frac{\alpha_s^2}{\pi^2} n_f \Delta \eta \left\{ \frac{1}{6N_c} \mu^{2\epsilon} B(1-\epsilon, 1-\epsilon) \left[\left(\frac{1}{\epsilon} - 3 + \frac{1}{2(1+\epsilon)} \right) \delta_{ij} + \frac{2\epsilon}{(1+\epsilon)} \frac{\Delta_i \Delta_j}{\Delta_\perp^2} \right] \frac{\Gamma(-2\epsilon)}{(\Delta_\perp^2)^{-2\epsilon}} \text{Tr}\{\partial_i U_x \partial_j U_x^\dagger\} \right. \\
 &\quad \left. + \frac{\mu^{2\epsilon}}{\epsilon} B(2-\epsilon, 2-\epsilon) \frac{\Gamma(-2\epsilon)}{(\Delta_\perp^2)^{-2\epsilon}} - \frac{1}{12\epsilon} \frac{\Gamma(-\epsilon)}{(\Delta_\perp^2)^{-\epsilon}} \right] U_x^{an} \partial_\perp^2 U_x^{ab}. \quad (22)
 \end{aligned}$$

The expression (22) should be compared to the light-cone expansion of the quark-loop part of the gluon propagator in an external field (see Fig. 7) performed in the Appendix A. A typical term of the light-cone expansion has the form:

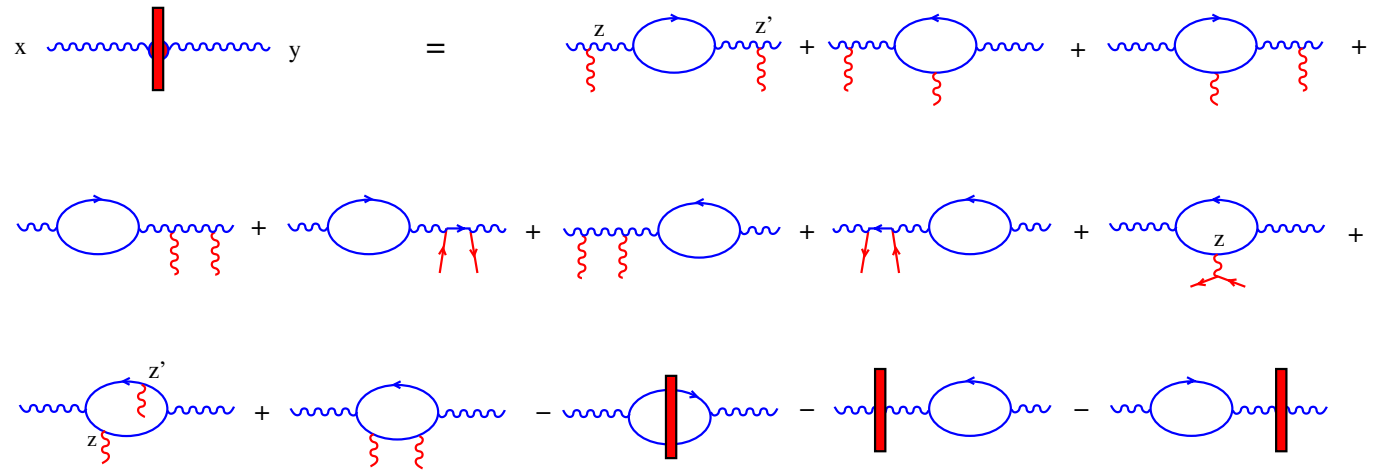


FIG. 7 (color online). A possible local contribution coming from the quark loop inside the shock wave.

$$\begin{aligned}
 A_{\bullet}^a(x_{*}, x_{\perp}) A_{\bullet}^b(y_{*}, y_{\perp}) &= \frac{ig^3}{16\pi^2} B(2 - \epsilon, 2 - \epsilon) \int_0^{\infty} \frac{d\alpha}{\alpha^3} \left(\frac{4i}{\alpha s} \right)^{\epsilon} \left(-\frac{i\alpha s}{4\pi\Delta_{*}} \right)^{1-\epsilon} e^{i(\Delta_{\perp}^2/4\Delta_{*})\alpha s} \left[-ig \int_{y_{*}}^{x_{*}} d\frac{2}{s} z_{*} \frac{1}{\epsilon} [(x-z)_{*}^{\epsilon}] \right. \\
 &+ (z-y)_{\perp}^{\epsilon} [(x_{*}, z_{*}]_x D^i G_{i\bullet}(z_{*}, x_{\perp}) [z_{*}, z'_{*}]_x [z_{*}, y_{*}]_x^{ab} + g62 \int_{y_{*}}^{x_{*}} d\frac{2}{s} z_{*} \int_{y_{*}}^{z_{*}} d\frac{2}{s} z'_{*} [(x_{*}, z_{*}]_x G_{i\bullet}^i(z_{*}, x_{\perp}) \\
 &\times [z_{*}, z'_{*}]_x G_{i\bullet}(z'_{*}, x_{\perp}) [z'_{*}, y_{*}]_x^{ab} \left. \left\{ \frac{1}{\epsilon} [(x-z)_{*}^{\epsilon} + (z'-y)_{*}^{\epsilon}] + (z-z')_{*}^{\epsilon} \right\} \right]. \quad (23)
 \end{aligned}$$

In our ‘‘external’’ field the characteristic distances z_{*}, z'_{*} are of the order of width of the shock wave: $z_{*}, z'_{*} \sim e^{\eta_2} \sqrt{s/m^2}$. As we shall see below, the characteristic distances x_{*} and y_{*} are $\sim e^{\eta_1} \sqrt{s/m^2}$ so we can neglect z_{*} and z'_{*} in comparison to x_{*} and/or y_{*} . The formula (23) simplifies to

$$\begin{aligned}
 A_{\bullet}^a(x_{*}, x_{\perp}) A_{\bullet}^b(y_{*}, y_{\perp}) &= \frac{ig^3}{16\pi^2} B(2 - \epsilon, 2 - \epsilon) \int_0^{\infty} \frac{d\alpha}{\alpha^3} \left(\frac{4i}{\alpha s} \right)^{\epsilon} \left(-\frac{i\alpha s}{4\pi\Delta_{*}} \right)^{1-\epsilon} e^{i(\Delta_{\perp}^2/4\Delta_{*})\alpha s} \left[-ig \frac{1}{\epsilon} \int_{y_{*}}^{x_{*}} d\frac{2}{s} z_{*} [x_{*}^{\epsilon} + (-y)_{*}^{\epsilon}] \right. \\
 &\times [(x_{*}, z_{*}]_x D^i G_{i\bullet}(z_{*}, x_{\perp}) [z_{*}, z'_{*}]_x [z_{*}, y_{*}]_x^{ab} + g^2 \int_{y_{*}}^{x_{*}} d\frac{2}{s} z_{*} \int_{y_{*}}^{z_{*}} d\frac{2}{s} z'_{*} [(x_{*}, z_{*}]_x G_{i\bullet}^i(z_{*}, x_{\perp}) \\
 &\times [z_{*}, z'_{*}]_x G_{i\bullet}(z'_{*}, x_{\perp}) [z'_{*}, y_{*}]_x^{ab} \left. \left\{ \frac{1}{\epsilon} [x_{*}^{\epsilon} + (-y)_{*}^{\epsilon}] + (z-z')_{*}^{\epsilon} \right\} \right]. \quad (24)
 \end{aligned}$$

A very important observation is that the contributions proportional to

$$g^4 n_f \int dz_{*} \int dz'_{*} \theta(z-z') (z-z')^{\epsilon} G_{i\bullet}(z_{*}) G_{i\bullet}(z'_{*}) \quad (25)$$

present in the individual diagrams in Fig. 11, cancel their sum. If it were not true, there would be an additional contribution to the gluon propagator (7) at the g^4 level coming from the small-size (large-momenta) quark loop. Indeed, the calculations of Feynman diagrams with the propagators (7) and (12) imply that we first take limit $z_{*}, z'_{*} \rightarrow 0$ and limit $d_{\perp} \rightarrow 2$ afterwards. With such order of limits, the contribution (25) vanishes. However, the proper order of these limits is to first take $d_{\perp} \rightarrow 2$ (which will give

finite expressions after adding the counterterms) and then try to impose condition that the external field is very narrow by taking the limit $z_{*}, z'_{*} \rightarrow 0$. In this case, Eq. (25) reduces to $g^4 n_f [GG]$. The noncommutativity of these limits would mean that the contribution $\frac{1}{p^2} [GG] \frac{1}{p^2}$ should be added to the gluon propagator (7) to restore the correct result. Fortunately, the terms $\sim (25)$ cancel which means that there are no additional contributions to the gluon propagator coming from the quark loop inside the shock wave (\equiv quark loop with large momenta).

Since there is no external field outside the shock wave, after cancellation of the terms $\sim (z-z')^{\epsilon}$ we see that at $x_{*} y_{*} > 0$ Eq. (24) vanishes, and at $x_{*} > 0 > y_{*}$ one can extend the limits of integration in the gluon operators to $\pm\infty$ and obtain

$$\begin{aligned}
 A_{\bullet}^a(x_{*}, x_{\perp}) A_{\bullet}^b(y_{*}, y_{\perp}) &= \frac{ig^2}{16\pi^2} B(2 - \epsilon, 2 - \epsilon) \int_0^{\infty} \frac{d\alpha}{\alpha^3} \left(\frac{4i}{\alpha s} \right)^{\epsilon} \left(-\frac{i\alpha s}{4\pi\Delta_{*}} \right)^{1-\epsilon} e^{i(\Delta_{\perp}^2/4\Delta_{*})\alpha s} \left[-ig \frac{1}{\epsilon} [x_{*}^{\epsilon} + (-y)_{*}^{\epsilon}] [DG]^{ab} \right. \\
 &+ g^2 [GG]^{ab} \left. \frac{1}{\epsilon} [x_{*}^{\epsilon} + (-y)_{*}^{\epsilon}] \right] \\
 &= \frac{ig^2}{16\pi^2} B(2 - \epsilon, 2 - \epsilon) \int_0^{\infty} \frac{d\alpha}{\alpha^3} \left(\frac{4i}{\alpha s} \right)^{\epsilon} \left(-\frac{i\alpha s}{4\pi\Delta_{*}} \right)^{1-\epsilon} e^{i(\Delta_{\perp}^2/4\Delta_{*})\alpha s} \frac{1}{\epsilon} [x_{*}^{\epsilon} + (-y)_{*}^{\epsilon}] \partial_{\perp}^2 U_x^{ab}. \quad (26)
 \end{aligned}$$

The light-cone expansion of gluon propagator contains only Wilson lines and their derivatives as should be expected after cancellation of the ‘‘contaminating’’ terms (25).

We have demonstrated in the Appendix A that the light-cone expansion of the quark-loop contribution to the gluon propagator coincides with Eq. (22) as should be expected once we established the commutativity of the limits $d_{\perp} \rightarrow 2$ and $z_{*}, z'_{*} \rightarrow 0$.

C. Quark loop in the coordinate representation

To calculate the integrals over momenta in Eq. (18) it is convenient to subtract (and add) $\text{Tr}\{t^a U_z t^b U_z^{\dagger}\}$ from $\text{Tr}\{t^a U_z t^b U_{z'}^{\dagger}\}$:

$$\begin{aligned}
 \text{Tr}\{t^a U_z t^b U_{z'}^{\dagger}\} &= \text{Tr}\{t^a U_z t^b U_{z'}^{\dagger} - t^a U_z t^b U_z^{\dagger}\} \\
 &+ \text{Tr}\{t^a U_z t^b U_z^{\dagger}\}. \quad (27)
 \end{aligned}$$

Let us start with the last term in the right-hand side of Eq. (27). In the momentum representation, this term corresponds to $\text{Tr}\{t^a U(q) t^b U^\dagger(q')\} \rightarrow 4\pi^2 \delta(q') \int dz e^{i(q,z)_\perp} \text{Tr}\{t^a U_z t^b U_z^\dagger\} = 2\pi^2 \delta(q') U^{ab}(q)$ so we get

$$\begin{aligned} & -2\alpha_s^2 n_f \Delta \eta t^a U_x \otimes t^b U_y^\dagger \frac{\mu^{2\epsilon}}{\pi} \int \tilde{d}^d p \tilde{d}^d q \frac{e^{i(p,x)_\perp - i(p-q,y)_\perp}}{p^2(p-q)^2} U^{ab}(q) \int_0^1 dv du \left[-\frac{\bar{u}u q^2 \Gamma(\epsilon)}{[(p-qu)^2 \bar{v}v + q^2 \bar{v}\bar{u}u]^\epsilon} \right. \\ & \left. + \frac{q^2 \bar{u}u \bar{v} \Gamma(1+\epsilon)}{[(p-qu)^2 \bar{v}v + q^2 \bar{v}\bar{u}u]^{1+\epsilon}} \{(p-qu)^2(-1+2v) + \bar{u}u q^2\} \right] \\ & = 2\frac{\alpha_s^2}{\pi} n_f \Delta \eta t^a U_x \otimes t^b U_y^\dagger \int \tilde{d}^d p \tilde{d}^d q \frac{e^{i(p,x)_\perp - i(p-q,y)_\perp}}{p^2(p-q)^2} U^{ab}(q) q^2 \frac{\Gamma(\epsilon)}{(q^2/\mu^2)^\epsilon} B(2-\epsilon, 2-\epsilon), \end{aligned} \quad (28)$$

where we have used integration by parts to transform the second term in the left-hand side of this equation. Alternatively, this result can be obtained directly from Eq. (15) after the substitution (27).

For future use we need to rewrite it in Schwinger's representation:

$$\begin{aligned} & -2\frac{\alpha_s^2}{\pi} \mu^{2-d} n_f \Delta \eta \{t^a U_x \otimes t^b U_y^\dagger\} \\ & \times \left(x \left| \frac{1}{p^2} \left(\frac{\Gamma(\epsilon)}{(-\partial^2)^\epsilon} \partial_\perp^2 U^{ab} \right) \frac{1}{p^2} \right| y \right) B(2-\epsilon, 2-\epsilon). \end{aligned} \quad (29)$$

The contribution coming from the first term in Eq. (27) is UV-finite. To calculate it in coordinate representation it is convenient to return back to the original expression

$$\begin{aligned} & -8\alpha_s^2 n_f \Delta \eta t^a U_x \otimes t^b U_y^\dagger \int \tilde{d}^2 k_1 \tilde{d}^2 k'_1 \tilde{d}^2 k_2 \tilde{d}^2 k'_2 \\ & \times e^{i(k_1, x-z)_\perp + i(k'_1, x-z')_\perp - i(k_2, y-z)_\perp - i(k'_2, y-z')_\perp} \\ & \times \text{Tr}\{t^a U_z t^b U_{z'}^\dagger - t^a U_z t^b U_{z'}^\dagger\} \\ & \times \int_0^1 du \frac{(k_1, k_2)(k'_1, k'_2) + (k_1, k'_1)(k_2, k'_2) - (k_1, k'_2)(k'_1, k_2)}{(k_1 + k'_1)^2 (k_2 + k'_2)^2 (k_1^2 u + k_1'^2 \bar{u})(k_2^2 u + k_2'^2 \bar{u})} \end{aligned}$$

and use the formulas

$$\begin{aligned} (U_x \otimes U_y^\dagger)^{\text{Fig.2a}} & = -\frac{\alpha_s^2}{2\pi^4} \Delta \eta \{t^a U_x \otimes t^b U_y^\dagger\} \int d^2 z d^2 z' \text{Tr}\{t^a U_z t^b U_{z'}^\dagger - t^a U_z t^b U_{z'}^\dagger\} \frac{1}{(z-z')^4} \left\{ 1 - \frac{(X, X')}{X^2 - X'^2} \ln \frac{X^2}{X'^2} \right. \\ & \left. - \frac{(Y, Y')}{Y^2 - Y'^2} \ln \frac{Y^2}{Y'^2} + \frac{(X, X')(Y, Y') + (X, Y)(X'Y') - (X, Y')(X'Y)}{X'^2 Y^2 - Y'^2 X^2} \ln \frac{X'^2 Y^2}{Y'^2 X^2} \right\} \\ & - 2\frac{\alpha_s^2}{\pi} \mu^{2\epsilon} B(2-\epsilon, 2-\epsilon) \Delta \eta \{t^a U_x \otimes t^b U_y^\dagger\} \left(x_\perp \left| \frac{1}{p_\perp^2} \left(\frac{\Gamma(\epsilon)}{(-\partial_\perp^2)^\epsilon} \partial_\perp^2 U \right) \frac{1}{p_\perp^2} \right| y_\perp \right). \end{aligned} \quad (32)$$

Sum of the UV-divergent contributions takes the form

$$2n_f \alpha_s^2 \frac{\mu^{2\epsilon}}{\pi} B(2-\epsilon, 2-\epsilon) \Delta \eta t^a U_x \otimes t^b U_y^\dagger \left(x_\perp \left| \frac{1}{p_\perp^2} \left\{ \frac{\Gamma(\epsilon)}{(p_\perp^2)^\epsilon}, \partial_\perp^2 U \right\} \frac{1}{p_\perp^2} - \frac{1}{p_\perp^2} \left(\frac{\Gamma(\epsilon)}{(-\partial_\perp^2)^\epsilon} \partial_\perp^2 U \right) \frac{1}{p_\perp^2} \right| y_\perp \right)^{ab}. \quad (33)$$

The counterterm is calculated in the Appendix A (we use the \overline{MS} scheme):

$$\begin{aligned} & \int \tilde{d}^d k_1 \tilde{d}^d k_2 \frac{(k_1, k_2) e^{i(k_1, x_1) + i(k_2, x_2)}}{(k_1 + k_2)^2 (k_1^2 \bar{u} + k_2^2 u)} \\ & = \frac{1}{4\pi^2 (x_1 - x_2)^2} \left[1 - \frac{(x_1, x_2)}{x_1^2 u + x_2^2 \bar{u}} \right] + O(d-2) \\ & \int \tilde{d}^d k_1 \tilde{d}^d k_2 \frac{k_{1i} k_{2j} - i \leftrightarrow j}{(k_1 + k_2)^2 (k_1^2 \bar{u} + k_2^2 u)} e^{i(k_1, x_1) + i(k_2, x_2)} \\ & = -\frac{x_{1i} x_{2j} - i \leftrightarrow j}{4\pi^2 (x_1 - x_2)^2 (x_1^2 u + x_2^2 \bar{u})} + O(d-2). \end{aligned} \quad (30)$$

After some algebra, one obtains:

$$\begin{aligned} U_x \otimes U_y^\dagger & = -\frac{\alpha_s^2}{2\pi^4} \Delta \eta \{t^a U_x \otimes t^b U_y^\dagger\} \\ & \times \int d^2 z d^2 z' \int_0^1 du \text{Tr}\{t^a U_z t^b U_{z'}^\dagger - t^a U_z t^b U_{z'}^\dagger\} \\ & \times \frac{1}{(z-z')^4} \left[1 - \frac{(X, X')}{X^2 u + X'^2 \bar{u}} - \frac{(Y, Y')}{Y^2 u + Y'^2 \bar{u}} \right. \\ & \left. + \frac{(X, X')(Y, Y') + (X, Y)(X'Y') - (X, Y')(X'Y)}{(X^2 u + X'^2 \bar{u})(Y^2 u + Y'^2 \bar{u})} \right], \end{aligned} \quad (31)$$

where $X \equiv x - z$, $X' \equiv x - z'$, $Y \equiv y - z$, $Y' \equiv y - z'$. Note that the singularity at $z' = z$ is integrable.

Performing the integration over u and adding the UV-divergent term (29) one obtains the total contribution of the diagram in Fig. 2(a) in the form:

$$- 2n_f \alpha_s^2 \Delta \eta t^a U_x \otimes t^b U_y^\dagger \frac{1}{3\pi\epsilon} \left(x_\perp \left| \frac{1}{p_\perp^2} \partial_\perp^2 U^{ab} \frac{1}{p_\perp^2} \right| y_\perp \right). \quad (34)$$

Adding the counterterm, one gets after some algebra

$$\begin{aligned} & n_f \frac{\alpha_s^2}{3\pi} \Delta \eta t^a U_x \otimes t^b U_y^\dagger \left(x_\perp \left| \frac{1}{p_\perp^2} \left[\left\{ \ln \frac{\mu^2}{p_\perp^2}, \partial_\perp^2 U \right\} - \left(\ln \frac{\mu^2}{-\partial_\perp^2} \partial_\perp^2 U \right) + \frac{5}{3} \partial_\perp^2 U \right] \frac{1}{p_\perp^2} \right| y_\perp \right)^{ab} \\ &= -n_f \frac{\alpha_s^2}{3\pi} \Delta \eta t^a U_x \otimes t^b U_y^\dagger \int \frac{d^2 z}{8\pi^2} \left\{ \frac{(x-y)^2}{X^2 Y^2} \left[\ln(x-y)^2 \mu^2 + \frac{5}{3} \right] - \frac{1}{X^2} \left[\ln Y^2 \mu^2 + \frac{5}{3} \right] \right. \\ & \quad \left. - \frac{1}{Y^2} \left[\ln X^2 \mu^2 + \frac{5}{3} \right] \right\} (2U_z - U_x - U_y)^{ab}. \end{aligned} \quad (35)$$

The calculation is simplified if one notes that $\partial_\perp^2 U_z$ in the l.h.s. can be replaced by $\partial_\perp^2 (U_z - \frac{1}{2}U_x - \frac{1}{2}U_y)$. Our final result for the sum of the diagrams in Fig. 2 has the form

$$\begin{aligned} (U_x \otimes U_y^\dagger)_{\text{Fig.2}} &= -\frac{\alpha_s^2}{2\pi^3} \Delta \eta n_f \{t^a U_x \otimes t^b U_y^\dagger\} \int dz \left[\frac{1}{\pi} \int dz' \text{Tr}^{\text{col}} \{t^a U_z t^b U_{z'}^\dagger - t^a U_z t^b U_z^\dagger\} \frac{1}{(z-z')^4} \left\{ 1 - \frac{(X, X')}{X^2 - X'^2} \ln \frac{X^2}{X'^2} \right. \right. \\ & \quad \left. \left. - \frac{(Y, Y')}{Y^2 - Y'^2} \ln \frac{Y^2}{Y'^2} + \frac{(X, X')(Y, Y') + (X, Y)(X'Y') - (X, Y')(X'Y)}{X'^2 Y^2 - Y'^2 X^2} \ln \frac{X'^2 Y^2}{Y'^2 X^2} \right\} \right. \\ & \quad \left. + \frac{1}{12} \left\{ \frac{(x-y)^2}{X^2 Y^2} \left[\ln(x-y)^2 \mu^2 + \frac{5}{3} \right] - \frac{1}{X^2} \left[\ln Y^2 \mu^2 + \frac{5}{3} \right] - \frac{1}{Y^2} \left[\ln X^2 \mu^2 + \frac{5}{3} \right] \right\} (2U_z - U_x - U_y)^{ab} \right]. \end{aligned} \quad (36)$$

As we mentioned above, the contribution of diagrams in Fig. 3 is obtained from Eq. (36) by replacement $t^a U_x \otimes t^b U_y^\dagger \rightarrow U_x t^b \otimes U_y^\dagger t^a$ and the contribution of the diagram in Fig. 4 can be obtained from Eq. (36) by taking $y = x$ in the integrand (and changing the sign)

$$\begin{aligned} (U_x \otimes U_y^\dagger)_{\text{Fig.4}} &= \frac{\alpha_s^2}{\pi^3} \Delta \eta n_f \{t^a U_x t^b \otimes U_y^\dagger\} \int dz \left[\frac{1}{\pi} \right. \\ & \quad \times \int dz' \text{Tr} \{t^a U_z t^b U_{z'}^\dagger - t^a U_z t^b U_z^\dagger\} \\ & \quad \times \frac{1}{(z-z')^4} \left(1 - \frac{(X, X')}{X^2 - X'^2} \ln \frac{X^2}{X'^2} \right) \\ & \quad \left. - \frac{1}{6X^2} \left[\ln X^2 \mu^2 + \frac{5}{3} \right] (U_z - U_x)^{ab} \right]. \end{aligned} \quad (37)$$

Similarly, the contribution of the diagram in Fig. 5 is obtained by the replacement $x \rightarrow y$:

$$\begin{aligned} (U_x \otimes U_y^\dagger)_{\text{Fig.5}} &= \frac{\alpha_s^2}{\pi^3} \Delta \eta n_f \{U_x \otimes t^b U_y^\dagger t^a\} \int dz \left[\frac{1}{\pi} \right. \\ & \quad \times \int dz' \text{Tr}^{\text{col}} \{t^a U_z t^b U_{z'}^\dagger - t^a U_z t^b U_z^\dagger\} \\ & \quad \times \frac{1}{(z-z')^4} \left(1 - \frac{(Y, Y')}{Y^2 - Y'^2} \ln \frac{Y^2}{Y'^2} \right) \\ & \quad \left. - \frac{1}{6Y^2} \left[\ln Y^2 \mu^2 + \frac{5}{3} \right] (U_z - U_y)^{ab} \right]. \end{aligned} \quad (38)$$

Summing the contributions of the diagrams in Fig. 2–5 and taking Tr over the color indices, one obtains

$$\begin{aligned} \text{Tr}\{U_x U_y^\dagger\} &= \frac{\alpha_s^2}{\pi^3} \Delta \eta n_f \text{Tr} \{t^a U_x t^b U_y^\dagger\} \int d^2 z \left[\frac{1}{\pi} \int d^2 z' \text{Tr} \{t^a U_z t^b U_{z'}^\dagger - t^a U_z t^b U_z^\dagger\} \frac{1}{(z-z')^4} \right. \\ & \quad \times \left\{ 1 - \frac{X'^2 Y^2 + Y'^2 X^2 - (x-y)^2 (z-z')^2}{2(X'^2 Y^2 - Y'^2 X^2)} \ln \frac{X'^2 Y^2}{Y'^2 X^2} \right\} \\ & \quad \left. + \frac{1}{12} \left\{ -\frac{(x-y)^2}{X^2 Y^2} \left[\ln(x-y)^2 \mu^2 + \frac{5}{3} \right] + \frac{X^2 - Y^2}{X^2 Y^2} \ln \frac{X^2}{Y^2} \right\} (2U_z - U_x - U_y)^{ab} \right]. \end{aligned} \quad (39)$$

Let us present the total result for the sum of the leading-order BK equation and the quark NLO correction

$$\begin{aligned}
\frac{d}{d\eta} \text{Tr}\{U_x U_y^\dagger\} &= \frac{\alpha_s}{2\pi^2} \int d^2z [\text{Tr}\{U_x U_z^\dagger\} \text{Tr}\{U_z U_y^\dagger\} - N_c \text{Tr}\{U_x U_y^\dagger\}] \left[\frac{(x-y)^2}{X^2 Y^2} \left(1 - \frac{\alpha_s n_f}{6\pi} \left[\ln(x-y)^2 \mu^2 + \frac{5}{3} \right] \right) \right. \\
&\quad \left. + \frac{\alpha_s n_f}{6\pi} \frac{X^2 - Y^2}{X^2 Y^2} \ln \frac{X^2}{Y^2} \right] + \frac{\alpha_s^2}{\pi^4} n_f \text{Tr}\{t^a U_x t^b U_y^\dagger\} \int d^2z d^2z' \text{Tr}\{t^a U_z t^b U_{z'}^\dagger - t^a U_{z'} t^b U_z^\dagger\} \frac{1}{(z-z')^4} \\
&\quad \times \left\{ 1 - \frac{X'^2 Y^2 + Y'^2 X^2 - (x-y)^2 (z-z')^2}{2(X'^2 Y^2 - Y'^2 X^2)} \ln \frac{X'^2 Y^2}{Y'^2 X^2} \right\}. \tag{40}
\end{aligned}$$

We see the first term proportional to $\ln(\dots)^2 \mu^2$ (we will call it the ‘‘UV’’ term) has the same structure as the zero-order contribution (3). In the next section we will use it to determine the argument of the running coupling constant in Eq. (3).

D. Comparison to NLO BFKL

To compare with the NLO BFKL equation we need to linearize Eq. (40) which gives

$$\begin{aligned}
\frac{d}{d\eta} \mathcal{U}(x, y) &= \frac{\alpha_s N_c}{2\pi^2} \int d^2z (\mathcal{U}(x, z) + \mathcal{U}(z, y) - \mathcal{U}(x, y)) \left[\frac{(x-y)^2}{X^2 Y^2} \left(1 - \frac{\alpha_s n_f}{6\pi} \left[\ln(x-y)^2 \mu^2 + \frac{5}{3} \right] \right) \right. \\
&\quad \left. + \frac{\alpha_s n_f}{6\pi} \frac{X^2 - Y^2}{X^2 Y^2} \ln \frac{X^2}{Y^2} \right] - \frac{\alpha_s^2 n_f}{4N_c \pi^4} \int d^2z d^2z' \frac{\mathcal{U}(z, z')}{(z-z')^4} \left\{ 1 - \frac{X'^2 Y^2 + Y'^2 X^2 - (x-y)^2 (z-z')^2}{2(X'^2 Y^2 - Y'^2 X^2)} \ln \frac{X'^2 Y^2}{Y'^2 X^2} \right\}. \tag{41}
\end{aligned}$$

This should be compared to the quark part of the nonforward BFKL kernel [18] but the Fourier transformation from the momentum space to the dipole-type representation appears to be rather difficult.

To simplify the comparison, let us consider the case of forward scattering and write down the Mellin representation of $\mathcal{U}(x, y)$

$$\mathcal{U}^\eta(x-y) = \int d\nu (x-y)^{2\nu} \mathcal{U}_\nu^\eta, \quad \gamma \equiv \frac{1}{2} + i\nu, \tag{42}$$

where we have displayed the dependence on the rapidity η explicitly. Using the integrals ($\chi(\gamma) \equiv [-\psi(\gamma) - \psi(1-\gamma) + 2\psi(1)]$)

$$\begin{aligned}
&\int d^2z \frac{(x-y)^2}{X^2 Y^2} [(X^2)^\gamma + (Y^2)^\gamma - ((x-y)^2)^\gamma] = 2\pi \chi(\gamma) ((x-y)^2)^\gamma, \\
&\int d^2z \left[\frac{\ln X^2/Y^2}{Y^2} - \frac{\ln X^2/Y^2}{X^2} \right] (X^{2\gamma} + Y^{2\gamma} - (x-y)^{2\gamma}) = \pi (x-y)^{2\gamma} \left\{ \psi'(1-\gamma) - \psi'(\gamma) - \chi^2(\gamma) + \frac{4}{\gamma} \chi(\gamma) \right\}, \\
&\int \frac{d^2z d^2z'}{(z-z')^{4-2\gamma}} \left\{ 1 - \frac{X'^2 Y^2 + Y'^2 X^2 - (x-y)^2 (z-z')^2}{2(X'^2 Y^2 - Y'^2 X^2)} \ln \frac{X'^2 Y^2}{Y'^2 X^2} \right\} = \frac{\pi^4 \cos \pi \gamma}{\sin^2 \pi \gamma} \frac{2 + 3\gamma(1-\gamma)}{(1-4\gamma^2)(3-2\gamma)} (x-y)^{2\gamma}, \tag{43}
\end{aligned}$$

we obtain

$$\begin{aligned}
\frac{d}{d\eta} \mathcal{U}_\nu^\eta &= \frac{\alpha_s N_c}{\pi} \left[1 - \frac{\alpha_s}{6\pi} n_f \ln(x-y)^2 \mu^2 \right] \left(\chi(\gamma) - \frac{\alpha_s}{12\pi} n_f \right. \\
&\quad \times \left[\psi'(\gamma) - \psi'(1-\gamma) + \chi^2(\gamma) - \frac{4}{\gamma} \chi(\gamma) \right] \\
&\quad \left. + \frac{10}{3} \chi(\gamma) + \frac{3\pi^2 \cos \pi \gamma}{N_c^2 \sin^2 \pi \gamma} \frac{2 + 3\gamma(1-\gamma)}{(1-4\gamma^2)(3-2\gamma)} \right) \mathcal{U}_\nu^\eta, \tag{44}
\end{aligned}$$

where $\gamma = \frac{1}{2} + i\nu$. This expression should be compared to the NLO BFKL result [19]. Unfortunately, there is no explicit expression for the coordinate-space NLO BFKL kernel yet. However, the last two terms in braces in right-hand side of this Equation coincide with the expression for the n_f part of the eigenvalue $\delta(\gamma)$ of Ref. [19]. The first

term in braces should correspond to the quark part of β -function contribution to the eigenvalue $\delta(\gamma)$. We expect to study the relation to NLO BFKL in detail after completing the calculation of the gluon loop.

IV. BUBBLE CHAIN AND THE ARGUMENT OF COUPLING CONSTANT

To get an argument of coupling constant we can trace the quark part of the β -function (proportional to n_f). In the leading log approximation the quark part of the β -function comes from the bubble chain of quark loops in the shock-wave background (cf. Ref. [20]). We can either have no intersection of quark loop with the shock wave (see Fig. 8) or we may have one of the loops in the shock-wave background. (See Fig. 9.)

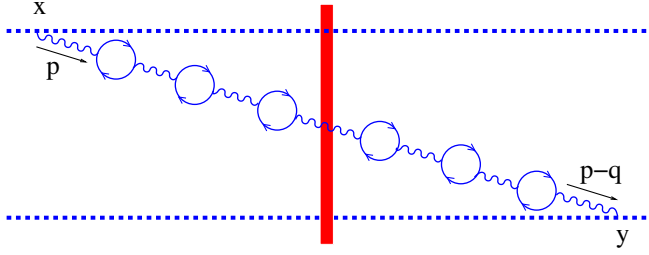


FIG. 8 (color online). Bubble chain without the quark-loop intersection with the shock wave.

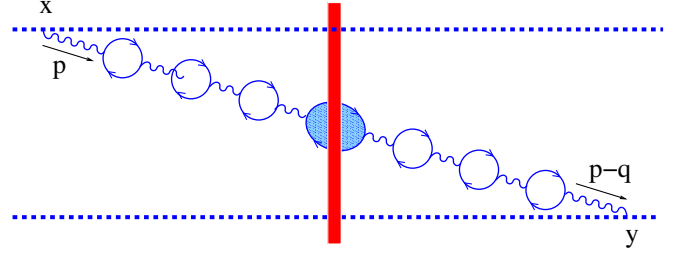


FIG. 9 (color online). Bubble chain with quark loop crossing the shock wave.

It is easy to see that the sum of these diagrams yields

$$\begin{aligned} \frac{d}{d\eta} \text{Tr}\{U_x U_y^\dagger\} &= 2\alpha_s \text{Tr}\{t^a U_x t^b U_y^\dagger\} \int d^2 p d^2 q [e^{i(p,x)_\perp} \\ &\quad - e^{i(p,y)_\perp}] [e^{-i(p-q,x)_\perp} - e^{-i(p-q,y)_\perp}] \\ &\quad \times \frac{1}{p^2 (1 + \frac{\alpha_s}{6\pi} \ln \frac{\mu^2}{p^2})} \left(1 - \frac{\alpha_s n_f}{6\pi} \ln \frac{q^2}{\mu^2}\right) \\ &\quad \times \partial_\perp^2 U^{ab}(q) \frac{1}{(p-q)^2 (1 + \frac{\alpha_s}{6\pi} \ln \frac{\mu^2}{(p-q)^2})}, \end{aligned} \quad (45)$$

where we have left only the UV part (29) of the quark loop. (In principle, one should also include the dressing of the UV-finite $1/N_c$ term in Eq. (41) by bubble chain, but I think that it is a separate contribution which has nothing to do with the argument of the BK equation). Replacing the quark part of the β -function $-\frac{\alpha_s}{6\pi} n_f \ln \frac{p^2}{\mu^2}$ by the total contribution $\frac{\alpha_s}{4\pi} b \ln \frac{p^2}{\mu^2}$ (where $b = \frac{11}{3N_c} - \frac{2}{3} n_f$), we get

$$\begin{aligned} \frac{d}{d\eta} \text{Tr}\{U_x U_y^\dagger\} &= 2 \text{Tr}\{t^a U_x t^b U_y^\dagger\} \int d^2 p d^2 q [e^{i(p,x)_\perp} \\ &\quad - e^{i(p,y)_\perp}] [e^{-i(p-q,x)_\perp} - e^{-i(p-q,y)_\perp}] \\ &\quad \times \frac{\alpha_s(p^2)}{p^2} \alpha_s^{-1}(q^2) \partial_\perp^2 U^{ab}(q) \frac{\alpha_s((p-q)^2)}{(p-q)^2}. \end{aligned} \quad (46)$$

To go to the coordinate space, let us expand the coupling constants in Eq. (46) in powers of $\alpha_s = \alpha_s(\mu^2)$, i.e. return back to Eq. (45) with $\frac{\alpha_s}{6\pi} n_f \rightarrow -b \frac{\alpha_s}{4\pi}$. In the first order we get the UV part of the NLO BK Eq. (40)

$$\begin{aligned} \frac{d}{d\eta} \text{Tr}\{U_x U_y^\dagger\} &= \frac{\alpha_s}{2\pi^2} \int d^2 z [\text{Tr}\{U_x U_z^\dagger\} \text{Tr}\{U_z U_y^\dagger\} \\ &\quad - N_c \text{Tr}\{U_x U_y^\dagger\}] \\ &\quad \times \left[\frac{(x-y)^2}{X^2 Y^2} \left(1 + b \frac{\alpha_s}{4\pi} \ln(x-y)^2 \mu^2\right) \right. \\ &\quad \left. - b \frac{\alpha_s}{4\pi} \frac{X^2 - Y^2}{X^2 Y^2} \ln \frac{X^2}{Y^2} \right]. \end{aligned} \quad (47)$$

In this section, we perform the calculations in the leading log approximation

$$\alpha_s \ln \frac{p^2}{\mu^2} \sim 1, \quad \alpha_s \ll 1 \quad (48)$$

[hence we omit the constant term ($\sim \frac{5}{3}$) from the Eq. (40)]. In the second order in the expansion we obtain

$$\begin{aligned} &- 2\alpha_s \int d^2 p d^2 q e^{i(p,x)_\perp - i(p-q,y)_\perp} \frac{1}{p^2 (1 - \frac{b\alpha_s}{4\pi} \ln \frac{\mu^2}{p^2})} \left(1 - \frac{b\alpha_s}{4\pi} \ln \frac{\mu^2}{q^2}\right) \partial_\perp^2 U^{ab}(q) \frac{1}{(p-q)^2 (1 - \frac{b\alpha_s}{4\pi} \ln \frac{\mu^2}{(p-q)^2})} \\ &= -\frac{b^2 \alpha_s^2}{8\pi^2} \left(x \left| \frac{\ln^2 \frac{\mu^2}{p^2}}{p^2} \partial_\perp^2 U \frac{1}{p^2} + \frac{\ln \frac{\mu^2}{p^2}}{p^2} \partial_\perp^2 U \frac{\ln \frac{\mu^2}{p^2}}{p^2} + \frac{1}{p^2} \partial_\perp^2 U \frac{\ln^2 \frac{\mu^2}{p^2}}{p^2} - \frac{\ln \frac{\mu^2}{p^2}}{p^2} \left(\ln \frac{\mu^2}{-\partial_\perp^2} \partial_\perp^2 U \right) \frac{1}{p^2} - \frac{1}{p^2} \left(\ln \frac{\mu^2}{-\partial_\perp^2} \partial_\perp^2 U \right) \frac{\ln \frac{\mu^2}{p^2}}{p^2} \right| y \right). \end{aligned}$$

Again, it is convenient to replace $\partial_\perp^2 U_z$ by $\partial_\perp^2 \tilde{U}_z$ where $\tilde{U}_z = U_z - \frac{U_x}{2} - \frac{U_y}{2}$:
Using the formulas

$$\begin{aligned}
& \left(x \left| -\ln^2 \frac{\mu^2}{p^2} \tilde{U} \frac{1}{p^2} - \frac{1}{p^2} \tilde{U} \ln^2 \frac{\mu^2}{p^2} + \ln \frac{\mu^2}{p^2} \left(\ln \frac{\mu^2}{-\partial_{\perp}^2} \tilde{U} \right) \frac{1}{p^2} + \frac{1}{p^2} \left(\ln \frac{\mu^2}{-\partial_{\perp}^2} \tilde{U} \right) \ln \frac{\mu^2}{p^2} - \ln \frac{\mu^2}{p^2} \tilde{U} \frac{\ln \frac{\mu^2}{p^2}}{p^2} - \frac{\ln \frac{\mu^2}{p^2}}{p^2} \tilde{U} \ln \frac{\mu^2}{p^2} \right| y \right) \\
& + \left(x \left| \frac{\ln \frac{\mu^2}{p^2}}{p^2} \right| y \right) \left[\left(\ln \frac{\mu^2}{-\partial_{\perp}^2} \tilde{U} \right)_x + \left(\ln \frac{\mu^2}{-\partial_{\perp}^2} \tilde{U} \right)_y \right] \\
& = \int dz \left[\frac{1}{4\pi^2 X^2} \left[\ln X^2 \mu^2 \ln Y^2 \mu^2 - \ln \frac{X^2}{Y^2} \ln \Delta^2 \mu^2 - \ln^2 \Delta^2 \mu^2 \right] \right. \\
& \quad \left. + \frac{1}{4\pi^2 Y^2} \left[\ln X^2 \mu^2 \ln Y^2 \mu^2 + \ln \frac{X^2}{Y^2} \ln \Delta^2 \mu^2 - \ln^2 \Delta^2 \mu^2 \right] \right] \left(U_z - \frac{1}{2} U_x - \frac{1}{2} U_y \right)
\end{aligned}$$

and

$$\begin{aligned}
& \left(x \left| 2 \frac{p_i \ln^2 \frac{\mu^2}{p^2}}{p^2} \tilde{U} \frac{p_i}{p^2} + 2 \frac{p_i \ln \frac{\mu^2}{p^2}}{p^2} \tilde{U} \frac{p_i \ln \frac{\mu^2}{p^2}}{p^2} + 2 \frac{p_i}{p^2} \tilde{U} \frac{p_i \ln^2 \frac{\mu^2}{p^2}}{p^2} - 2 \frac{p_i \ln \frac{\mu^2}{p^2}}{p^2} \left(\ln \frac{\mu^2}{-\partial_{\perp}^2} U \right) \frac{p_i}{p^2} - 2 \frac{p_i}{p^2} \left(\ln \frac{\mu^2}{-\partial_{\perp}^2} U \right) \frac{p_i \ln \frac{\mu^2}{p^2}}{p^2} \right| y \right) \\
& = \int \frac{dz}{4\pi^2} \left(U_z - \frac{1}{2} U_x - \frac{1}{2} U_y \right) \left\{ \left[\frac{1}{X^2} + \frac{1}{Y^2} \right] \ln^2 \Delta^2 \mu^2 + \frac{\Delta^2}{X^2 Y^2} \left[-\ln^2 \Delta^2 \mu^2 + \frac{2\Delta_i}{\pi \Delta^2} \int dr \left[\frac{r_i Y^2 - (Y, r) Y_i}{r^2 (Y - r)^2} \ln(r - X)^2 \right. \right. \right. \\
& \quad \left. \left. \left. - \frac{r_i X^2 - (X, r) X_i}{r^2 (X - r)^2} \ln(r - Y)^2 \right] \right] \right\}, \tag{49}
\end{aligned}$$

we obtain

$$\begin{aligned}
\frac{d}{d\eta} \text{Tr}\{U_x U_y^\dagger\}^{(2)} &= \frac{\alpha_s}{2\pi^2} \left(\frac{b\alpha_s}{4\pi} \right)^2 \int d^2 z \left[\text{Tr}\{U_x U_z^\dagger\} \text{Tr}\{U_z U_y^\dagger\} - N_c \text{Tr}\{U_x U_y^\dagger\} \right] \left[\frac{(x-y)^2}{X^2 Y^2} \ln^2(x-y)^2 \mu^2 + \frac{1}{X^2} \ln \frac{X^2}{Y^2} \right. \\
& \quad \left. \times (\ln X^2 \mu^2 + \ln(x-y)^2 \mu^2) - \frac{1}{Y^2} \ln \frac{X^2}{Y^2} (\ln Y^2 \mu^2 + \ln(x-y)^2 \mu^2) \right]. \tag{50}
\end{aligned}$$

We have omitted the contribution of the last integral in right-hand side of Eq. (49) since it is negligible in the limits $X \gg Y$, $Y \gg X$ and $X, Y \gg x - y$, and therefore can be dropped in the leading log approximation (48). Adding the first-order contribution [first line in the Eq. (40)], we get

$$\begin{aligned}
\frac{d}{d\eta} \text{Tr}\{U_x U_y^\dagger\} &= \frac{\alpha_s}{2\pi^2} \int d^2 z \left[\text{Tr}\{U_x U_z^\dagger\} \text{Tr}\{U_z U_y^\dagger\} - N_c \text{Tr}\{U_x U_y^\dagger\} \right] \left\{ \frac{(x-y)^2}{X^2 Y^2} \left[1 + \frac{b\alpha_s}{4\pi} \ln(x-y)^2 \mu^2 \right. \right. \\
& \quad \left. \left. + \left(\frac{b\alpha_s}{4\pi} \right)^2 \ln^2(x-y)^2 \mu^2 \right] + \frac{b\alpha_s}{4\pi} \frac{1}{X^2} \ln \frac{X^2}{Y^2} \left[1 + \frac{b\alpha_s}{4\pi} \ln(x-y)^2 \mu^2 + \frac{b\alpha_s}{4\pi} \ln X^2 \mu^2 \right] \right\} \\
& \quad - \frac{b\alpha_s}{4\pi} \frac{1}{Y^2} \ln \frac{X^2}{Y^2} \left[1 + \frac{b\alpha_s}{4\pi} \ln(x-y)^2 \mu^2 + \frac{b\alpha_s}{4\pi} \ln Y^2 \mu^2 \right]. \tag{51}
\end{aligned}$$

Our guess for the argument of the coupling constant in all orders in $\ln p^2/\mu^2$ is [21]

$$\begin{aligned}
\frac{d}{d\eta} \text{Tr}\{U_x U_y^\dagger\} &= \frac{\alpha_s((x-y)^2)}{2\pi^2} \\
& \times \int d^2 z \left[\text{Tr}\{U_x U_z^\dagger\} \text{Tr}\{U_z U_y^\dagger\} \right. \\
& \quad \left. - N_c \text{Tr}\{U_x U_y^\dagger\} \right] \left[\frac{(x-y)^2}{X^2 Y^2} + \frac{1}{X^2} \right. \\
& \quad \left. \times \left(\frac{\alpha_s(X^2)}{\alpha_s(Y^2)} - 1 \right) + \frac{1}{Y^2} \left(\frac{\alpha_s(Y^2)}{\alpha_s(X^2)} - 1 \right) \right]. \tag{52}
\end{aligned}$$

We see now that the argument of the coupling constant in

the BK equation is size of the original dipole $(x-y)^2$ as it was advertised in Eq. (5).

Actually, since the each of the quark loops gives $\ln(x_y)_\perp^2 \mu^2 + \frac{5}{3}$ coming from $B(2-\epsilon, 2-\epsilon)$ in Eq. (17), it is natural [14] to include this 5/3 correction in the argument of coupling constant which will give $\alpha_s(e^{5/3}(x-y)_\perp^2)$ in the right-hand side of Eq. (52).

V. CONCLUSIONS AND OUTLOOK

First, there are no new operators at the one-loop level—just as at the tree level, the high-energy scattering can be described in terms of Wilson lines. The fact that there are no new operators at the one-loop level is rather remarkable. In the case of the usual light-cone operator expansion this is not true; for example, if we have the operator

$$\begin{aligned}
 [GG] = & \int dudv\theta(u-v)[\infty p_1, up_1]_x G_{\bullet i}(up_1 + x_\perp) \\
 & \times [up_1, vp_1]_x G_{\bullet i}(vp_1 + x_\perp)[vp_1, -\infty p_1]_x
 \end{aligned} \quad (53)$$

in the leading order, one should expect the operator

$$\begin{aligned}
 \alpha_s \int dudv\theta(u-v) \ln(u-v) [\infty p_1, up_1]_x G_{\bullet i}(up_1 + x_\perp) \\
 \times [up_1, vp_1]_x G_{\bullet i}(vp_1 + x_\perp)[vp_1, -\infty p_1]_x
 \end{aligned} \quad (54)$$

in the NLO (in general, any new loop brings an additional factor $\alpha_s \ln(u-v)$). This does not happen here, and in addition the operator $[GG]$ appears only in the combination $-i[DG] + [GG] = \partial_\perp^2 U$, exactly as at the tree level. I have checked this by the explicit calculation of the quark-loop contribution and expect to confirm it by the calculation of the gluon loop.

Second conclusion of the paper is that the argument of the coupling constant in the BK equation (obtained from the renormalon-based arguments) appears to be the size of the parent dipole rather than the size of produced dipoles.

It should be mentioned that in the recent paper [16] the NLO BK equation is rewritten in terms of three effective coupling constants. This is a different extrapolation of \ln^2 result (51) to all orders, see the discussion in the Appendix B.

I have obtained the result for the argument of the coupling constant in the nonlinear evolution of dipoles using the quark part of the β -function. It is necessary to confirm this result by calculating the diagrams with gluon loops. Also, it would be extremely interesting to check how (and if) this argument of the coupling constant arises from the correlation function of the original dipole and the ‘‘diamond’’ high-energy effective action [22] formulated in terms of the (renorm-invariant) Wilson lines. The study is in progress.

ACKNOWLEDGMENTS

The author is indebted to Yu. Kovchegov for numerous discussions and for informing about the results of similar calculation [16] prior to the publication. (The NLO result (40) in Ref. [16] is the same but the interpretation of the argument of the coupling constant is different, see the discussion in the Appendix B). The author would like to thank E. Iancu and other members of theory group at CEA Saclay for valuable discussions and kind hospitality. This work was supported by Contract No. DE-AC05-06OR23177 under which the Jefferson Science Associates, LLC operate the Thomas Jefferson National Accelerator Facility.

APPENDIX A: LIGHT-CONE EXPANSION OF THE QUARK-LOOP CONTRIBUTION TO GLUON PROPAGATOR IN THE BACKGROUND FIELD

The expression (22) should be compared to the light-cone expansion of the quark-loop part of the gluon propagator in an external field. The quark-loop contribution to the propagator of a gluon in the external field has the form:

$$\begin{aligned}
 A_\bullet^m(x)A_\bullet^n(y) = & \int dx'dy' \left(x \left| \frac{1}{P^2 g_{\bullet\mu} + 2iG_{\bullet\mu} + \mathcal{O}_{\bullet\mu}} \right| x' \right)^{ma} \\
 & \times \text{Tr} \left[t^a \gamma_\mu \left(x' \left| \frac{1}{\not{p}} \right| y' \right) t^b \gamma_\nu \left(y' \left| \frac{1}{\not{p}} \right| x' \right) \right] \\
 & \times \left(y' \left| \frac{1}{P^2 g_{\nu\bullet} + 2iG_{\nu\bullet} + \mathcal{O}_{\nu\bullet}} \right| y \right)^{bn}, \quad (A1)
 \end{aligned}$$

where

$$\mathcal{O}_{\mu\bullet} = \mathcal{O}_{\bullet\mu} = \frac{1}{\alpha} D^i G_{i\mu} = \frac{2p_{2\mu}}{\alpha s} D^i G_{i\bullet}. \quad (A2)$$

An additional term in the gluon propagator is due to the fact that the external gluon field of the target satisfies the Yang-Mills equation with a source $D^\mu G_{\mu\nu}^a = -g\bar{\psi}\gamma_\nu t^a\psi$. From the viewpoint of Feynman diagrams in the bF gauge, this term comes from the diagrams with the quark insertions shown in Fig. 10 (in the lightlike gauge this term arises automatically, see Ref. [9]). For the contribution $\sim \mathcal{O}_{\mu\bullet}$ the quark propagator reduces to

$$\begin{aligned}
 \gamma_\mu t^a \frac{(\beta_p + \beta_k)\not{p}_2 + (\not{p} + \not{k})_\perp}{(\alpha_p + \alpha_k)(\beta_p + \beta_k)s - (p+k)_\perp^2} t^b \not{p}_2 \\
 - t^b \not{p}_1 \frac{(\beta_p - \beta_k)\not{p}_2 + (\not{p} - \not{k})_\perp}{(\alpha_p - \alpha_k)(\beta_p - \beta_k)s - (p-k)_\perp^2} t^a \gamma_\mu. \quad (A3)
 \end{aligned}$$

As explained in Ref. [1] at $\alpha_k \ll \alpha_p$ one can shift the contour of integration over β_p away from the pole in the denominators in the above equation. After that $\beta_p \sim \frac{p_\perp^2}{\alpha_p s}$ so one can neglect the terms proportional to transverse momenta in the denominator and in the numerator. One obtains

$$\frac{1}{\alpha s} \gamma_\mu \not{p}_2 \not{p}_1 t^a t^b - t^b t^a \not{p}_1 \not{p}_2 \gamma_\mu \simeq \frac{1}{\alpha} i f^{abc} t^c \gamma_\mu, \quad (A4)$$

which corresponds to the vertex of the insertion of $\mathcal{O}_{\mu\bullet}$ operator.

We need to expand the Eq. (A1) near the light cone $x \rightarrow y$ and compare it to the light-cone expansion of the same propagator in the shock-wave background (refvesvkladlikone). The technique for the light-cone expansion

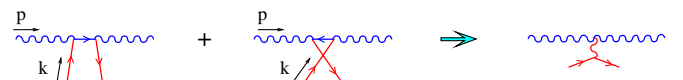


FIG. 10 (color online). ‘‘Target’’ contribution to the gluon propagator in the external field.

sion of propagators in external fields was developed in Refs. [23,24]). The expansion of the tree-level quark propagator has the form [24]:

$$\begin{aligned}
\left(x' \left| \frac{1}{\not{p}} \right| y'\right) &= \frac{\not{A}\Gamma(2-\epsilon)}{2\pi^2(-\Delta^2)^{2-\epsilon}} + \frac{\Gamma(1-\epsilon)}{16\pi^2(-\Delta^2)^{1-\epsilon}} \int_0^1 du \left\{ \bar{u}\not{A}\sigma G(x_u) + u\sigma G(x_u)\not{A} - 2i\bar{u}u\not{A}D^\lambda G_{\lambda\Delta} \right. \\
&+ 4\not{A} \int_0^u dv \bar{u}v G_\Delta^\xi(x_u) G_{\Delta\xi}(x_v) \left. \right\} + \frac{\Gamma(-\epsilon)}{16\pi^2(-\Delta^2)^{-\epsilon}} \int_0^1 du \left\{ i\left(\frac{1}{2} - \bar{u}u\right) D^\lambda G_{\lambda\rho} \gamma^\rho + \frac{i}{2} \bar{u}u(1-2u)\hat{D}D^\lambda G_{\lambda\Delta} \right. \\
&- \bar{u}u(1-2u)\gamma^\rho [G_\Delta^\xi(x_u), G_{\rho\xi}(x_u)] - \frac{1}{2} \bar{u}u \epsilon_{\Delta\mu\nu\lambda} D^\mu D_\xi G^{\xi\nu} \gamma^\lambda \gamma_5 + i\frac{\bar{u}u}{2} ([G_{\Delta\xi}(x_u), \tilde{G}_v^\xi(x_u)] \\
&+ [\tilde{G}_{\Delta\xi}(x_u), G_v^\xi(x_u)]) \gamma_\nu \gamma_5 + \int_0^u dv \left[\left(\bar{u} - 2\bar{u}v - \frac{1}{2}\right) G_{\Delta\xi}(x_u) G^{\lambda\xi}(x_v) \gamma_\lambda + \left(v - 2\bar{u}v - \frac{1}{2}\right) G^{\lambda\xi}(x_u) G_{\Delta\xi}(x_v) \gamma_\lambda \right. \\
&\left. + \frac{i}{2} (1 - 2\bar{u} - 2v) G_{\Delta\xi}(x_u) \tilde{G}^{\lambda\xi}(x_v) \gamma_\lambda \gamma_5 - \frac{i}{2} \tilde{G}_{\Delta\xi}(x_u) G^{\lambda\xi}(x_v) \gamma_\lambda \gamma_5 \right] \left. \right\} + O(\text{twist } 3) \quad (\text{A5})
\end{aligned}$$

where $\Delta = x' - y'$ and $\epsilon = 1 - \frac{d_1}{2}$. Hereafter, we use the notations $x_u \equiv ux' + \bar{u}y'$ and $G_{\Delta\mu} \equiv G_{\alpha\mu}\Delta^\alpha$ for brevity [25].

We need to multiply this by similar expansion for the antiquark propagator. The product of the two quark propagators has the form:

$$\text{Tr } t^a \gamma^\alpha \left(x' \left| \frac{1}{\not{p}} \right| y'\right) t^b \gamma^\beta \left(y' \left| \frac{1}{\not{p}} \right| x'\right) = (\tilde{T}_1)_{\alpha\beta}^{ab} + (\tilde{T}_2)_{\alpha\beta}^{ab} + (\tilde{T}_3)_{\alpha\beta}^{ab}, \quad (\text{A6})$$

where

$$\begin{aligned}
(\tilde{T}_1)_{\alpha\beta}^{ab} &= i \frac{B(2-\epsilon, 2-\epsilon)}{4\pi^2} [x', y']^{ab} \left(x' \left| (p^2 g_{\alpha\beta} - p_\alpha p_\beta) \frac{\Gamma(\epsilon)}{(-p^2)^\epsilon} \right| y'\right) + \frac{B(2-\epsilon, 1-\epsilon)}{8\pi^4} \frac{\Gamma(3-2\epsilon)}{(-\Delta^2)^{3-2\epsilon}} \int_0^1 du ([x', x_u] \\
&\times (2i\bar{u}\Delta_\alpha G_{\beta\Delta}(x_u) - 2iu\Delta_\beta G_{\alpha\Delta}(x_u) + i\Delta^2 G_{\alpha\beta}(x_u)) [x_u, y']^{ab}, \quad (\text{A7})
\end{aligned}$$

$$\begin{aligned}
(\tilde{T}_2)_{\alpha\beta}^{ab} &= i \frac{B(2-\epsilon, 1-\epsilon)}{8\pi^4} \frac{\Gamma(3-2\epsilon)}{(-\Delta^2)^{3-2\epsilon}} \int_0^1 du \bar{u}u (2\Delta_\alpha \Delta_\beta - \Delta^2 g_{\alpha\beta}) ([x', x_u] D^\lambda G_{\lambda\Delta}(x_u) [x_u, y']^{ab} \\
&+ \frac{B(2-\epsilon, -\epsilon)}{16\pi^4} \frac{\Gamma(2-2\epsilon)}{(\Delta^2)^{2-2\epsilon}} \int_0^1 du ([x', x_u] \left[\left[-i\left(\frac{1}{2} - \bar{u}u\right) D^\lambda G_{\lambda\alpha}(x_u) \Delta_\beta - \frac{i}{2} \bar{u}u(1-2u) D_\alpha D^\lambda G_{\lambda\Delta}(x_u) \Delta_\beta \right. \right. \\
&\left. \left. + \alpha \leftrightarrow \beta \right] + i\left(\frac{1}{2} - \bar{u}u\right) g_{\alpha\beta} D^\lambda G_{\lambda\Delta}(x_u) + \frac{i}{2} \bar{u}u(1-2u) g_{\alpha\beta} (\Delta \cdot D) D^\lambda G_{\lambda\Delta}(x_u) \right] [x_u, y']^{ab}, \quad (\text{A8})
\end{aligned}$$

$$\begin{aligned}
(\tilde{T}_3)_{\alpha\beta}^{ab} &= -(2\Delta_\alpha \Delta_\beta - \Delta^2 g_{\alpha\beta}) \frac{B(2-\epsilon, 1-\epsilon)}{2\pi^4} \frac{\Gamma(3-2\epsilon)}{(-\Delta^2)^{3-2\epsilon}} \int_0^1 dudv \text{Tr} \{ \bar{u}v \theta(u-v) t^b [y', x'] t^a [x', x_u] G_{\Delta\xi}(x_u) \\
&\times [x_u, x_v] G_{\Delta\xi}^\xi(x_v) [x_v, y'] + u\bar{v}\theta(v-u) t^a [x', y'] t^b [y', x_u] G_{\Delta\xi}(x_u) [x_u, x_v] G_{\Delta\xi}^\xi(x_v) [x_v, x'] \} \\
&+ \frac{B(2-\epsilon, -\epsilon)}{16\pi^4} \frac{\Gamma(2-\epsilon)}{(-\Delta^2)^{2-\epsilon}} \int_0^1 dudv \text{Tr} \left\{ -2(\Delta_\alpha \delta_\beta^\lambda + \Delta_\beta \delta_\alpha^\lambda - g_{\alpha\beta} \Delta^\lambda) \left(\theta(u-v) t^b [y', x'] t^a [x', x_u] \right. \right. \\
&\times \left. \left\{ \left(\bar{u} - 2\bar{u}v - \frac{1}{2}\right) G_{\Delta\xi}(x_u) [x_u, x_v] G_{\lambda\xi}^\xi(x_v) + \left(v - 2\bar{u}v - \frac{1}{2}\right) G_{\lambda\xi}^\xi(x_u) [x_u, x_v] G_{\Delta\xi}(x_v) \right\} [x_v, y'] \right. \\
&+ \left. \theta(v-u) t^a [x', y'] t^b [y', x_u] \left\{ \left(u - 2\bar{u}u - \frac{1}{2}\right) G_{\Delta\xi}(x_u) [x_u, x_v] G_{\lambda\xi}^\xi(x_v) + \left(\bar{v} - 2\bar{v}u - \frac{1}{2}\right) G_{\lambda\xi}^\xi(x_u) [x_u, x_v] G_{\Delta\xi}(x_v) \right\} \right. \\
&\times \left. [x_v, x'] \right\} - \frac{B(1-\epsilon, 1-\epsilon)}{16\pi^4} \frac{\Gamma(2-2\epsilon)}{(\Delta^2)^{2-2\epsilon}} \int_0^1 dudv \text{Tr} \{ \Delta^2 t^a ([x', x_u] G_{\alpha\xi}(x_u) [x_u, y'] t^b [y', x_v] G_{\beta\xi}^\xi(x_v) [x_v, x'] \\
&+ \alpha \leftrightarrow \beta) + 2(\bar{u}v + \bar{v}u) t^a (g_{\alpha\beta} [x', x_u] G_{\Delta\xi}(x_u) [x_u, y] t^b [y', x_v] G_{\Delta\xi}^\xi(x_v) [x_v, x] \\
&- [x', x_u] (G_{\Delta\alpha}(x_u) [x_u, y] t^b [y', x_v] G_{\Delta\beta}(x_v) + \alpha \leftrightarrow \beta) [x_v, x'] \\
&- 2\bar{u}\Delta_\alpha t^a [x', x_u] G_{\Delta\xi}(x_u) [x_u, y'] t^b [y', x_v] G_{\beta\xi}^\xi(x_v) [x_v, x'] - 2\bar{v}\Delta_\alpha t^a [x', x_u] G_{\beta\xi}(x_u) [x_u, y'] t^b [y', x_v] G_{\Delta\xi}^\xi(x_v) [x_v, x'] \\
&- 2u\Delta_\beta t^a [x', x_u] G_{\Delta\xi}(x_u) [x_u, y'] t^b [y', x_v] G_{\alpha\xi}^\xi(x_v) [x_v, x'] - 2v\Delta_\beta t^a [x', x_u] G_{\alpha\xi}(x_u) [x_u, y'] t^b [y', x_v] G_{\Delta\xi}^\xi(x_v) [x_v, x'] \}, \quad (\text{A9})
\end{aligned}$$

where we have omitted terms $\sim \epsilon_{\alpha\beta\mu\nu} \Delta^\mu(\dots)^\nu$ and $[G_{\Delta\xi}, G_{\nu^\xi}]$ which do not contribute to Eq. (A1) with our accuracy.

Next we need to substitute the product (A6) into the expression (A1). Since we will integrate the expression (A1) over x_* and y_* (to get $U_x U_y^\dagger$) we can neglect the terms proportional to $P_\alpha(\dots)_\beta$ and $(\dots)_\alpha P_\beta$. Indeed, using the identity

$$P_\alpha \frac{1}{P^2 g_{\alpha\beta} + 2iG_{\alpha\beta}} = \frac{1}{P^2} P_\beta + \frac{1}{P^2} D^\mu G_{\mu\alpha} \times \frac{1}{P^2 g_{\alpha\beta} + 2iG_{\alpha\beta}}, \quad (\text{A10})$$

we get

$$P_\alpha \frac{1}{P^2 g_{\alpha\bullet} + 2iG_{\alpha\bullet} + \mathcal{O}_{\alpha\bullet}} = \frac{1}{P^2} P_\bullet, \quad (\text{A11})$$

$$\frac{1}{P^2 g_{\bullet\alpha} + 2iG_{\bullet\alpha} + \mathcal{O}_{\bullet\alpha}} P_\alpha = P_\bullet \frac{1}{P^2}.$$

As explained in Ref. [1], one can drop the terms proportional to P_\bullet since they lead to the terms proportional to the integral of total derivative, namely

$$\int dx_* \left[\infty p_1, \frac{2}{s} x_* p_1 \right] t^a \left[\frac{2}{s} x_* p_1, -\infty p_1 \right] \times \left(D_\bullet \Phi \left(\frac{2}{s} x_* p_1, \dots \right) \right)_{ab} = \int dx_* \frac{d}{dx_*} \left\{ \left[\infty p_1, \frac{2}{s} x_* p_1 \right] t^a \left[\frac{2}{s} x_* p_1, -\infty p_1 \right] \times \left(\Phi \left(\frac{2}{s} x_* p_1, \dots \right) \right)_{ab} \right\} = 0. \quad (\text{A12})$$

Using this property one can rewrite Eq. (A6) in the form

$$\text{Tr } t^a \gamma^\alpha \left(x' \left| \frac{1}{\not{p}} \right| y' \right) t^b \gamma^\beta \left(y' \left| \frac{1}{\not{p}} \right| x' \right) \Leftrightarrow (T_1)_{\alpha\beta}^{ab} + (T_2)_{\alpha\beta}^{ab} + (T_3)_{\alpha\beta}^{ab}, \quad (\text{A13})$$

where

$$(T_1)_{\alpha\beta}^{ab} = ig_{\alpha\beta} \frac{\Gamma^2(2-\epsilon)}{4\pi^2 \Gamma(4-2\epsilon)} \left(x \left| P^2 \frac{\Gamma(\epsilon)}{(-P^2)^\epsilon} \right| y \right)^{ab} - \frac{g\Gamma^2(2-\epsilon)}{4\pi^4 \Gamma(3-2\epsilon)} \left(x \left| \frac{\Gamma(\epsilon)}{(-p^2)^\epsilon} \right| y \right) \int_0^1 du ([x', x_u] G_{\alpha\beta}(x_u) [x_u, y'])^{ab}$$

$$+ \frac{ig}{8\pi^2} \frac{\Gamma(3-\epsilon)\Gamma(1-\epsilon)}{\Gamma(4-2\epsilon)} \left(x \left| \frac{\Gamma(\epsilon)p_\rho}{(-p^2)^\epsilon} \right| y \right) \int_0^1 du ([x', x_u] [\bar{u} \delta_\alpha^\rho G_{\Delta\beta}(x_u) - u \delta_\beta^\rho G_{\Delta\alpha}(x_u)] [x_u, y'])^{ab}$$

$$(T_2)_{\alpha\beta}^{ab} = g_{\alpha\beta} (1-2\epsilon) \frac{g\Gamma^2(2-\epsilon)}{4\pi^2 \Gamma(4-2\epsilon)} \left(x \left| \frac{\Gamma(1+\epsilon)}{(-p^2)^{1+\epsilon}} \right| y \right) \int_0^1 du ([x', x_u] D^\mu G_{\mu\Delta}^{ab}(x_u) [x_u, y'])^{ab} + (\tilde{T}_2)_{\alpha\beta}^{ab}$$

$$(T_3)_{\alpha\beta}^{ab} = ig_{\alpha\beta} (1-2\epsilon) \frac{g^2 \Gamma^2(2-\epsilon)}{2\pi^2 \Gamma(4-2\epsilon)} \left(x \left| \frac{\Gamma(1+\epsilon)}{(-p^2)^{1+\epsilon}} \right| y \right) \int_0^1 du \int_0^u dv \bar{u} v ([x', x_u] G_{\Delta\xi}(x_u) [x_u, x_v] G_{\Delta}^\xi(x_v) [x_v, y'])^{ab} + (\tilde{T}_3)_{\alpha\beta}^{ab}, \quad (\text{A14})$$

and \Leftrightarrow means ‘‘equal up to the contributions $\sim P_\alpha(\dots)_\beta$ and $(\dots)_\alpha P_\beta$.’’

Next we expand the propagator (A1) near the light cone. The first contribution comes from the T_1 term which represents diagrams in Fig. 11(a)–11(g). The calculation yields

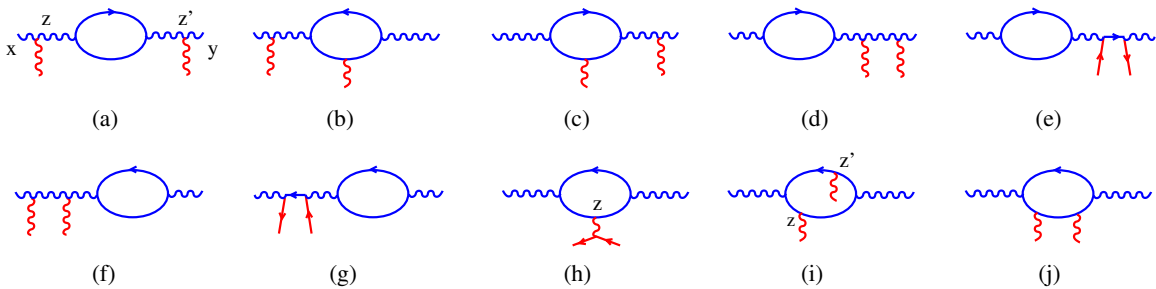


FIG. 11 (color online). Quark-loop contribution to the gluon propagator in an external field.

$$\begin{aligned}
& \int dx' dy' \left(x \left| \frac{1}{P^2 g_{\bullet\mu} + 2iG_{\bullet\mu} + \mathcal{O}_{\bullet\mu}} \right| x' \right)^{ma} T_{1\alpha\beta}^{ab} \left(y' \left| \frac{1}{P^2 g_{\nu\bullet} + 2iG_{\nu\bullet} + \mathcal{O}_{\nu\bullet}} \right| y \right)^{bn} \\
&= \frac{1}{8\pi^2} B(2-\epsilon, 2-\epsilon) \left(x \left| \frac{1}{p^2} \left[\frac{\partial_{\perp}^2 U^{ab}}{\alpha}, \frac{\Gamma(\epsilon)}{(-p^2)^\epsilon} \right] \frac{1}{p^2} \right| y \right) - \frac{ig}{4\pi^2} B(2-\epsilon, 2-\epsilon) \left(x \left| \frac{1}{p^2} \left[\frac{D^i G_{\bullet}^{ab}}{\alpha}, \frac{\Gamma(\epsilon)}{(-p^2)^\epsilon} \right] \frac{1}{p^2} \right| y \right) \\
&+ \frac{g^2 \Gamma^2(1-\epsilon)}{32\pi^2 \Gamma(4-2\epsilon)} \int_0^\infty \frac{d\alpha}{\alpha^3} \int_{y_*}^{x_*} d\frac{2}{s} z_* \int_{y_*}^{z_*} d\frac{2}{s} z'_* ([x_*, z_*]_x G_{\bullet i}(z_*, x_{\perp}) [z_*, z'_*]_x G_{\bullet j}(z'_*, x_{\perp}) [z'_*, y_*]_x)^{ab} \left(\frac{4i}{\alpha s} \right)^\epsilon \\
&\times \left\{ g_{ij} \left[\frac{1}{\epsilon} [(2-\epsilon)(x-z')_*^\epsilon - (x-z)_*^\epsilon - (z-z')_*^\epsilon] + \frac{1}{\epsilon} [(2-\epsilon)(z-y)_*^\epsilon - (z'-y)_*^\epsilon - (z-z')_*^\epsilon] + 2(z-z')_*^\epsilon \right. \right. \\
&- 2(2-\epsilon) \frac{(z-z')_*}{(x-z')_*^{1-\epsilon}} + (1-\epsilon) \frac{(z-z')_*^2}{(x-z')_*^{2-\epsilon}} - 2(2-\epsilon) \frac{(z-z')_*}{(z-y)_*^{1-\epsilon}} + (1-\epsilon) \frac{(z-z')_*^2}{(z-y)_*^{2-\epsilon}} + \frac{2(1-\epsilon)}{3-\epsilon} (z-z')_*^2 \\
&\times [\Delta_*^{-2+\epsilon} + (z-z')_*^{-2+\epsilon} - (x-z)_*^{-2+\epsilon} - (z'-y)_*^{-2+\epsilon}] \left. \right] + \frac{1}{(1+\epsilon)} [(x-z)_*^{1+\epsilon} + (z-z')_*^{1+\epsilon} - (x-z')_*^{1+\epsilon} \\
&+ (1+\epsilon) \frac{(x-z)_*(z-z')_*}{(x-z')_*^{1-\epsilon}} + (z'-y)_*^{1+\epsilon} + (z-z')_*^{1+\epsilon} - (z-y)_*^{1+\epsilon} + (1+\epsilon) \frac{(z-z')_*(z'-i)_*}{(x-z')_*^{1-\epsilon}} \left. \right] \left(\frac{3-\epsilon}{\Delta_*} g_{ij} \right. \\
&+ i \frac{\alpha s}{4\Delta_*^2} [\Delta_{\perp}^2 g_{ij} - \Delta_i \Delta_j] \left. \right) + \frac{g_{ij}}{\epsilon} (1-\epsilon)(3-2\epsilon) [2(z-z')_*^\epsilon + (x-z)_*^\epsilon + (z-y)_*^\epsilon - 2(x-z')_*^\epsilon - 2(z'-y)_*^\epsilon] \left. \right\} \\
&\times \left(-\frac{i\alpha s}{4\pi\Delta_*} \right)^{1-\epsilon} e^{i(\Delta_{\perp}^2/4\Delta_*)\alpha s}. \tag{A15}
\end{aligned}$$

In our external field the characteristic distances z_* (z'_*) are of the order of width of the shock wave: $z_*, z'_* \sim e^{\eta_2} \sqrt{s/m^2}$. As we shall see below, the characteristic distances x_* and y_* are $\sim e^{\eta_2} \sqrt{s/m^2}$ so we can neglect z_* and z'_* in comparison to x_* and/or y_* . The formula (A15) simplifies to

$$\begin{aligned}
& \int dx' dy' \left(x \left| \frac{1}{P^2 g_{\bullet\mu} + 2iG_{\bullet\mu} + \mathcal{O}_{\bullet\mu}} \right| x' \right)^{ma} T_{1\alpha\beta}^{ab} \left(y' \left| \frac{1}{P^2 g_{\nu\bullet} + 2iG_{\nu\bullet} + \mathcal{O}_{\nu\bullet}} \right| y \right)^{bn} \\
&= \frac{1}{8\pi^2} B(2-\epsilon, 2-\epsilon) \left(x \left| \frac{1}{p^2} \left[\frac{\partial_{\perp}^2 U^{ab}}{\alpha}, \frac{\Gamma(\epsilon)}{(-p^2)^\epsilon} \right] \frac{1}{p^2} \right| y \right) + \frac{ig^3}{16\pi^2} \frac{B(2-\epsilon, 2-\epsilon)}{\epsilon} \int_0^\infty \frac{d\alpha}{\alpha^3} \left(\frac{4i}{\alpha s} \right)^\epsilon [x_*^\epsilon + (-y)_*^\epsilon] \\
&\times \left(-\frac{i\alpha s}{4\pi\Delta_*} \right)^{1-\epsilon} e^{i(\Delta_{\perp}^2/4\Delta_*)\alpha s} \int_{y_*}^{x_*} d\frac{2}{s} z_* ([x_*, z_*]_x D^i G_{\bullet i}(z_*, x_{\perp}) [z_*, z'_*]_x [z_*, y_*]_x)^{ab} + \frac{g^2 \Gamma(1-\epsilon) \Gamma(2-\epsilon)}{16\pi^2 \Gamma(4-2\epsilon)} \int_0^\infty \frac{d\alpha}{\alpha^3} \\
&\times \int_{y_*}^{x_*} d\frac{2}{s} z_* \int_{y_*}^{z_*} d\frac{2}{s} z'_* ([x_*, z_*]_x G_{\bullet i}(z_*, x_{\perp}) [z_*, z'_*]_x G_{\bullet i}(z'_*, x_{\perp}) [z'_*, y_*]_x)^{ab} \left(\frac{4i}{\alpha s} \right)^\epsilon \left\{ -\frac{1-\epsilon}{\epsilon} [x_*^\epsilon + (-y)_*^\epsilon - 2(z-z')_*^\epsilon] \right. \\
&+ \left. \frac{1}{3-\epsilon} (z-z')_*^\epsilon \right\} \left(-\frac{i\alpha s}{4\pi\Delta_*} \right)^{1-\epsilon} e^{i(\Delta_{\perp}^2/4\Delta_*)\alpha s}. \tag{A16}
\end{aligned}$$

The term $\sim T_2$ coming from the diagram in Fig. 11(h) has the form

$$\begin{aligned}
& \int dx' dy' \left(x \left| \frac{1}{p^2} \right| x' \right) T_{2\bullet\bullet}^{ab} \left(y' \left| \frac{1}{p^2} \right| y \right) = -\frac{i}{32\pi^2} \int_0^\infty \frac{d\alpha}{\alpha^3} \left(\frac{i}{\alpha s} \right)^\epsilon \left(-\frac{i\alpha s}{4\pi\Delta_*} \right)^{1-\epsilon} e^{i(\Delta_{\perp}^2/4\Delta_*)\alpha s} \frac{\Gamma(2-\epsilon)\Gamma(1-\epsilon)}{\Gamma(3-2\epsilon)} \\
&\times \left\{ \frac{(4-\epsilon)(1-\epsilon)}{\epsilon(2-\epsilon)(3-\epsilon)} [x_*^\epsilon + (-y)_*^\epsilon - \Delta_*^\epsilon - \epsilon x_* y_* \Delta_*^{\epsilon-2}] - \frac{2(2-2\epsilon+\epsilon^2)}{\epsilon(2-\epsilon)(1-\epsilon^2)} \right. \\
&\times \left[\frac{1-\epsilon}{\Delta_*} + \frac{i\alpha s \Delta_{\perp}^2}{4\Delta_*^2} \right] \left[x_*^{1+\epsilon} + (-y)_*^{1+\epsilon} - \Delta_*^{1+\epsilon} - \frac{(1+\epsilon)x_* y_*}{\Delta_*^{1-\epsilon}} \right] \\
&- \frac{1}{\epsilon(1-\epsilon)(2+\epsilon)} \left[\frac{(2-\epsilon)(1-\epsilon)}{\Delta_*^2} + \frac{i(2-\epsilon)\alpha s}{2\Delta_*^3} \Delta_{\perp}^2 - \frac{\alpha^2 s^2}{16\Delta_*^4} \Delta_{\perp}^4 \right] \\
&\times [x_*^{2+\epsilon} + (-y)_*^{2+\epsilon} - \Delta_*^{2+\epsilon} - (2+\epsilon)x_* y_* \Delta_*^\epsilon] \left. \right\} \\
&\times \int_{y_*}^{x_*} d\frac{2}{s} z_* ([x_*, z_*]_x D^\lambda G_{\lambda\bullet}(z_*, x_{\perp}) [z_*, y_*]_x)^{ab}, \tag{A17}
\end{aligned}$$

where we have neglected z_* in comparison to x_* , y_* as discussed above. Since there is no field outside the shock wave [26],

at $x_* y_* > 0$ the contribution (A17) vanishes and at $x_* > 0, y_* < 0$ one can extend the limits of integration over z_* to $\pm\infty$ and get

$$\begin{aligned}
 \int dx' dy' \left(x \left| \frac{1}{p^2} \right| x' \right) T_{2\bullet\bullet}^{ab} \left(y' \left| \frac{1}{p^2} \right| y \right) \stackrel{x_* > 0 > y_*}{=} & -\frac{i}{32\pi^2} \int_0^\infty \frac{d\alpha}{\alpha^3} \left(\frac{i}{\alpha s} \right)^\epsilon \left(-\frac{i\alpha s}{4\pi\Delta_*} \right)^{1-\epsilon} e^{i(\Delta_\perp^2/4\Delta_*)\alpha s} \frac{\Gamma(2-\epsilon)\Gamma(1-\epsilon)}{\epsilon\Gamma(3-2\epsilon)} \\
 & \times \left\{ \frac{(4-\epsilon)(1-\epsilon)}{(2-\epsilon)(3-\epsilon)} [x_*^\epsilon + (-y)_*^\epsilon - \Delta_*^\epsilon - \epsilon x_* y_* \Delta_*^{\epsilon-2}] - \frac{2(2-2\epsilon+\epsilon^2)}{(2-\epsilon)(1-\epsilon^2)} \right. \\
 & \times \left[\frac{1-\epsilon}{\Delta_*} + \frac{i\alpha s \Delta_\perp^2}{4\Delta_*^2} \right] \left[x_*^{1+\epsilon} + (-y)_*^{1+\epsilon} - \Delta_*^{1+\epsilon} - \frac{(1+\epsilon)x_* y_*}{\Delta_*^{1-\epsilon}} \right] \\
 & - \frac{1}{(1-\epsilon)(2+\epsilon)} \left[\frac{(2-\epsilon)(1-\epsilon)}{\Delta_*^2} + \frac{i(2-\epsilon)\alpha s}{2\Delta_*^3} \Delta_\perp^2 - \frac{\alpha^2 s^2}{16\Delta_*^4} \Delta_\perp^4 \right] \\
 & \left. \times [x_*^{2+\epsilon} + (-y)_*^{2+\epsilon} - \Delta_*^{2+\epsilon} - (2+\epsilon)x_* y_* \Delta_*^\epsilon] \right\} [DG]_{\mathbf{x}}^{ab}, \tag{A18}
 \end{aligned}$$

where $[DG]$ is defined by Eq. (21). Similarly, the integral $\int_{y_*}^{x_*} d\frac{2}{s} z_* ([x_*, z_*]_{\mathbf{x}} D^\lambda G_{\lambda\bullet}(z_*, x_\perp)$ in the second term in the right-hand side of Eq. (A16) can be reduced to $[DG]_{\mathbf{x}}$. The case $x_* < 0, y_* > 0$ is obtained from (A18) by the substitution $x \leftrightarrow y$.

The contribution of diagrams in Fig. 11(i) and 11(j) is

$$\begin{aligned}
 \int dx' dy' \left(x \left| \frac{1}{p^2} \right| x' \right) T_{3\bullet\bullet}^{ab} \left(y' \left| \frac{1}{p^2} \right| y \right) = & \frac{g^2}{16\pi^2} B(1-\epsilon, 2-\epsilon) \int_0^\infty \frac{d\alpha}{\alpha^3} \left(\frac{4i}{\alpha s} \right)^\epsilon \left(-\frac{i\alpha s}{4\pi\Delta_*} \right)^{1-\epsilon} e^{i(\Delta_\perp^2/4\Delta_*)\alpha s} \int_{y_*}^{x_*} d\frac{2}{s} z_* \\
 & \times \int_{y_*}^{z_*} d\frac{2}{s} z'_* \left(\left\{ \frac{(4-\epsilon)(1-\epsilon)}{\epsilon(2-\epsilon)(3-\epsilon)} [x_*^\epsilon + (-y)_*^\epsilon - \Delta_*^\epsilon - (z-z')^\epsilon] \right. \right. \\
 & - \frac{(z-z')^\epsilon}{(2-\epsilon)(3-\epsilon)} - \frac{(4-\epsilon)(1-\epsilon)x_* y_*}{(2-\epsilon)(3-\epsilon)\Delta_*^{2-\epsilon}} - \left. \left[\frac{1-\epsilon}{\Delta_*} + \frac{i\alpha s \Delta_\perp^2}{4\Delta_*^2} \right] \frac{2(2-2\epsilon+\epsilon^2)}{\epsilon(1-\epsilon^2)(2-\epsilon)} \right. \\
 & \times [x_*^{1+\epsilon} + (-y)_*^{1+\epsilon} - \Delta_*^{1+\epsilon} - (1+\epsilon)x_* y_* \Delta_*^{\epsilon-1}] - \left. \left[\frac{(2-\epsilon)(1-\epsilon)}{\Delta_*^2} \right. \right. \\
 & \left. \left. + \frac{i(2-\epsilon)\alpha s}{2\Delta_*^3} \Delta_\perp^2 - \frac{\alpha^2 s^2}{16\Delta_*^4} \Delta_\perp^4 \right] \frac{[x_*^{2+\epsilon} + (-y)_*^{2+\epsilon} - \Delta_*^{2+\epsilon} - (2+\epsilon)x_* y_* \Delta_*^\epsilon]}{\epsilon(1-\epsilon)(2+\epsilon)} \right\} \\
 & \times ([x_*, z_*]_{\mathbf{x}} G_{\bullet i}(z_*, x_\perp) [z_*, z'_*]_{\mathbf{x}} G_{\bullet}^i(z'_*, x_\perp) [z'_*, y_*]^{ab} + \left\{ -g_{ij} \frac{x_* y_*}{\Delta_*^{2-\epsilon}} \right. \\
 & - 2 \left[\frac{1-\epsilon}{\Delta_*} + \frac{i\alpha s \Delta_\perp^2}{4\Delta_*^2} \right] g_{ij} \frac{2-2\epsilon+\epsilon^2}{\epsilon(1-\epsilon^2)(2-\epsilon)} [x_*^{1+\epsilon} + (-y)_*^{1+\epsilon} - \Delta_*^{1+\epsilon} \\
 & - (1+\epsilon)x_* y_* \Delta_*^{\epsilon-1}] - \left. \left[\frac{(2-\epsilon)(1-\epsilon)}{\Delta_*^2} + \frac{i(2-\epsilon)\alpha s}{2\Delta_*^3} \Delta_\perp^2 - \frac{\alpha^2 s^2}{16\Delta_*^4} \Delta_\perp^4 \right] \right. \\
 & \times \frac{[x_*^{2+\epsilon} + (-y)_*^{2+\epsilon} - \Delta_*^{2+\epsilon} - (2+\epsilon)x_* y_* \Delta_*^\epsilon]}{\epsilon(1-\epsilon)(2+\epsilon)} g_{ij} - \left. \left[\frac{1-\epsilon}{\Delta_*} + \frac{i\alpha s \Delta_\perp^2}{4\Delta_*^2} \right] \right. \\
 & \times g_{ij} \frac{x_*^{1+\epsilon} + (-y)_*^{1+\epsilon} - \Delta_*^{1+\epsilon}}{\epsilon(1+\epsilon)} - \left. \left[2 \frac{g_{ij}}{\Delta_*} - \frac{i\alpha s}{\Delta_*^2} \Delta_i \Delta_j \right] \right. \\
 & \times \frac{x_*^{1+\epsilon} + (-y)_*^{1+\epsilon} - \Delta_*^{1+\epsilon} - (1+\epsilon)x_* y_* \Delta_*^{\epsilon-1}}{(1-\epsilon^2)(2-\epsilon)} \left. \right\} [x_*, z_*]^{am} 2 \text{Tr} \{ t^m G_{\bullet i}(z_*, x_\perp) \\
 & \times [z_*, z'_*] t^n G_{\bullet j}(z'_*, x_\perp) [z'_*, z_*]_{\mathbf{x}} + m \leftrightarrow n \} [z_*, y_*]^{nb}. \tag{A19}
 \end{aligned}$$

The final expression for the light-cone expansion of the quark-loop contribution to gluon propagator in the sum of the expressions (A16), (A17), and (A19). A very important observation is that the contributions proportional to

$$g^4 n_f \int dz_* \int dz'_* \theta(z-z')(z-z')^\epsilon G_{\bullet i}(z_*) G_{\bullet i}(z'_*) \tag{A20}$$

present in the Eqs. (A16) and (A19) cancel in their sum. If it were not true, there would be an additional contribution to the

gluon propagator (7) at the g^4 level coming from the small-size (large-momenta) quark loop. Indeed, the calculations of Feynman diagrams with the propagators (7) and (12) implies that we first take limit $z_*, z'_* \rightarrow 0$ and limit $d_\perp \rightarrow 2$ afterwards. With such order of limits, the contribution (A20) vanishes. However, the proper order of these limits is to take at first $d_\perp \rightarrow 2$ (which will give finite expressions after adding the counterterms) and then try to impose the condition that the external field is very narrow by taking the limit $z_*, z'_* \rightarrow 0$. In this case, Eq. (A20) reduces to $g^4 n_f [GG]$. The noncommutativity of these limits would

mean that the contribution $\frac{1}{p^2} [GG] \frac{1}{p^2}$ should be added to the gluon propagator (7) to restore the correct result. Fortunately, the terms \sim (A20) cancel which means that there are no additional contributions to the gluon propagator coming from the quark loop inside the shock wave (\equiv quark loop with large momenta).

Since there is no external field outside the shock wave, after cancellation of the terms $\sim (z - z')^\epsilon$ we see that at $x_* y_* > 0$ the sum of Eq. (A16) and (A19) vanishes, and at $x_* > 0 > y_*$ one can extend the limits of integration in the gluon operators to $\pm\infty$ and obtain

$$\int_{y_*}^{x_*} dz_* \int_{y_*}^{x_*} dz'_* ([x_*, z_*]_x G_{\bullet i}(z_*, x_\perp) [z_*, z'_*]_x G_{\bullet i}(z'_*, x_\perp) [z'_*, y_*]_x)^{ab} \rightarrow [GG]_x^{ab}, \quad (\text{A21})$$

$$\int_{y_*}^{x_*} dz_* \int_{y_*}^{z_*} dz'_* [x_*, z_*]^{am} \text{Tr}\{t^m G_{\bullet i}(z_*, x_\perp) [z_*, z'_*] t^n G_{\bullet j}(z'_*, x_\perp) [z'_*, z_*]_x + m \leftrightarrow n\} [z_*, y_*]_x^{nb} \rightarrow \text{Tr}\{t^a \partial_i U_x t^b \partial_j U_x^\dagger\}.$$

We get

$$\int dx' dy' \left(x \left| \frac{1}{P^2 g_{\bullet\alpha} + 2iG_{\bullet\alpha} + \mathcal{O}_{\bullet\alpha}} \right| x' \right)^{ma} (T_{1\alpha\beta}^{ab} + T_{2\alpha\beta}^{ab} + T_{3\alpha\beta}^{ab}) \left(y' \left| \frac{1}{P^2 g_{\beta\bullet} + 2iG_{\beta\bullet} + \mathcal{O}_{\beta\bullet}} \right| y \right)^{bn}$$

$$\stackrel{x_* > 0 > y_*}{=} \frac{1}{8\pi^2} B(2 - \epsilon, 2 - \epsilon) \left(x \left| \frac{1}{p^2} \left\{ \frac{\partial_\perp^2 U^{ab}}{\alpha}, \frac{\Gamma(\epsilon)}{(-p^2)^\epsilon} \right\} \frac{1}{p^2} \right| y \right) + \frac{g^2}{32\pi^2} B(1 - \epsilon, 2 - \epsilon) \int_0^\infty \frac{d\alpha}{\alpha^3} \left(\frac{4i}{\alpha s} \right)^\epsilon \left(-\frac{i\alpha s}{4\pi\Delta_*} \right)^{1-\epsilon}$$

$$\times e^{i(\Delta_\perp^2/4\Delta_*)\alpha s} \left(\left[-\frac{1-\epsilon}{\epsilon(3-2\epsilon)} [x_*^\epsilon + (-y)_*^\epsilon] + \frac{(4-\epsilon)(1-\epsilon)}{\epsilon(2-\epsilon)(3-\epsilon)} [x_*^\epsilon + (-y)_*^\epsilon - \Delta_*^\epsilon - \epsilon x_* y_* \Delta_*^{\epsilon-2}] \right. \right.$$

$$- \left. \left[\frac{1-\epsilon}{\Delta_*} + \frac{i\alpha s \Delta_\perp^2}{4\Delta_*^2} \right] \frac{2(2-2\epsilon+\epsilon^2)}{\epsilon(1-\epsilon^2)(2-\epsilon)} [x_*^{1+\epsilon} + (-y)_*^{1+\epsilon} - \Delta_*^{1+\epsilon} - (1+\epsilon)x_* y_* \Delta_*^{\epsilon-1}] \right.$$

$$- \left. \left[\frac{(2-\epsilon)(1-\epsilon)}{\Delta_*^2} + \frac{i(2-\epsilon)\alpha s}{2\Delta_*^3} \Delta_\perp^2 - \frac{\alpha^2 s^2}{16\Delta_*^4} \Delta_\perp^4 \right] \frac{[x_*^{2+\epsilon} + (-y)_*^{2+\epsilon} - \Delta_*^{2+\epsilon} - (2+\epsilon)x_* y_* \Delta_*^\epsilon]}{\epsilon(1-\epsilon)(2+\epsilon)} \right] \partial_\perp^2 U_x^{ab}$$

$$+ \left\{ -\frac{x_* y_*}{\Delta_*^{2-\epsilon}} - 2 \left[\frac{1-\epsilon}{\Delta_*} + \frac{i\alpha s \Delta_\perp^2}{4\Delta_*^2} \right] \frac{2-2\epsilon+\epsilon^2}{\epsilon(1-\epsilon^2)(2-\epsilon)} [x_*^{1+\epsilon} + (-y)_*^{1+\epsilon} - \Delta_*^{1+\epsilon} - (1+\epsilon)x_* y_* \Delta_*^{\epsilon-1}] \right.$$

$$- \left. \left[\frac{(2-\epsilon)(1-\epsilon)}{\Delta_*^2} + \frac{i(2-\epsilon)\alpha s}{2\Delta_*^3} \Delta_\perp^2 - \frac{\alpha^2 s^2}{16\Delta_*^4} \Delta_\perp^4 \right] \frac{[x_*^{2+\epsilon} + (-y)_*^{2+\epsilon} - \Delta_*^{2+\epsilon} - (2+\epsilon)x_* y_* \Delta_*^\epsilon]}{\epsilon(1-\epsilon)(2+\epsilon)} \right.$$

$$- \left. \left[\frac{1-\epsilon}{\Delta_*} + \frac{i\alpha s \Delta_\perp^2}{4\Delta_*^2} \right] \frac{x_*^{1+\epsilon} + (-y)_*^{1+\epsilon} - \Delta_*^{1+\epsilon}}{\epsilon(1+\epsilon)} - \frac{2}{\Delta_*} \frac{x_*^{1+\epsilon} + (-y)_*^{1+\epsilon} - \Delta_*^{1+\epsilon} - (1+\epsilon)x_* y_* \Delta_*^{\epsilon-1}}{(1-\epsilon^2)(2-\epsilon)} \right\} 4 \text{Tr}\{t^a \partial_i U_x t^b \partial_j U_x^\dagger\}$$

$$+ \frac{i\alpha s}{\Delta_*^2} \Delta^i \Delta^j \frac{x_*^{1+\epsilon} + (-y)_*^{1+\epsilon} - \Delta_*^{1+\epsilon} - (1+\epsilon)x_* y_* \Delta_*^{\epsilon-1}}{(1-\epsilon^2)(2-\epsilon)} 4 \text{Tr}\{t^a \partial_i U_x t^b \partial_j U_x^\dagger\}. \quad (\text{A22})$$

We see that the light-cone expansion of gluon propagator contains only Wilson lines and their derivatives as should be expected after cancellation of the contaminating terms (A20).

Next, to get the expansion of $[\infty, 0]_x \otimes [0, -\infty]_y$ near the light cone we integrate the expression (A22) over x_* from 0 to ∞ and over y_* from $-\infty$ to 0. It is easy to demonstrate that

$$\int_0^\infty dx_* \int_{-\infty}^0 dy_* \left(-\frac{i\alpha s}{4\pi\Delta_*} \right)^{1-\epsilon} e^{i(\Delta_\perp^2/4\Delta_*)\alpha s} \left\{ \frac{(4-\epsilon)(1-\epsilon)}{\epsilon(2-\epsilon)(3-\epsilon)} [x_*^\epsilon + (-y)_*^\epsilon - \Delta_*^\epsilon - \epsilon x_* y_* \Delta_*^{\epsilon-2}] \right.$$

$$- \frac{2(2-2\epsilon+\epsilon^2)}{\epsilon(2-\epsilon)(1-\epsilon^2)} \left[\frac{1-\epsilon}{\Delta_*} + \frac{i\alpha s \Delta_\perp^2}{4\Delta_*^2} \right] \left[x_*^{1+\epsilon} + (-y)_*^{1+\epsilon} - \Delta_*^{1+\epsilon} - \frac{(1+\epsilon)x_* y_*}{\Delta_*^{1-\epsilon}} \right] - \frac{1}{\epsilon(1-\epsilon)(2+\epsilon)}$$

$$\times \left. \left[\frac{(2-\epsilon)(1-\epsilon)}{\Delta_*^2} + \frac{i(2-\epsilon)\alpha s}{2\Delta_*^3} \Delta_\perp^2 - \frac{\alpha^2 s^2}{16\Delta_*^4} \Delta_\perp^4 \right] [x_*^{2+\epsilon} + (-y)_*^{2+\epsilon} - \Delta_*^{2+\epsilon} - (2+\epsilon)x_* y_* \Delta_*^\epsilon] \right\} = 0$$

(in particular, it means that the term (A18) coming from the diagram in Fig. 11(h) does not contribute). The result of the

integration of Eq. (A22) has the form

$$\begin{aligned}
 [\infty, 0]_x \otimes [0, -\infty]_y \xrightarrow{x_\perp \rightarrow y_\perp} &= \frac{2\alpha_s^2}{\pi} \Delta \eta B(2 - \epsilon, 2 - \epsilon) \left(x_\perp \left| \frac{1}{p_\perp^2} \left[\partial_\perp^2 U^{ab}, \frac{\Gamma(\epsilon)}{(p_\perp^2)^\epsilon} \right] \frac{1}{p_\perp^2} \right| y_\perp \right) + \frac{\alpha_s^2}{8\pi^2} \Delta \eta B(1 - \epsilon, 1 - \epsilon) \\
 &\times \frac{\Gamma(-1 - 2\epsilon)}{(\Delta_\perp^2)^{-1-2\epsilon}} \left(\left[-\frac{(4 - \epsilon)(1 - \epsilon)}{6\epsilon(1 + \epsilon)} + \frac{7 + \epsilon}{6(1 + \epsilon)} - \frac{1}{3(1 + \epsilon)(2 + \epsilon)} \right] \text{Tr}\{t^a \partial_i U_x t^b \partial_i U_x^\dagger\} \right. \\
 &\left. - \frac{2(1 + 2\epsilon)}{3(1 + \epsilon)(2 + \epsilon)} \frac{\Delta_i \Delta_j}{\Delta_\perp^2} \text{Tr}\{t^a \partial_i U_x t^b \partial_j U_x^\dagger\} \right) \quad (\text{A23})
 \end{aligned}$$

and therefore

$$\begin{aligned}
 \partial_i^x [\infty, 0]_x \otimes \partial_i^y [0, -\infty]_y \\
 \xrightarrow{x_\perp \rightarrow y_\perp} &\frac{\alpha_s^2 \Delta \eta}{\pi^2} \frac{B(2 - \epsilon)}{\epsilon} \frac{\Gamma(-2\epsilon)}{(\Delta_\perp^2)^{-2\epsilon}} \partial_\perp^2 U_x^{ab} \\
 &+ \frac{\alpha_s^2 \Delta \eta}{4\pi^2} B(1 - \epsilon) \frac{\Gamma(-2\epsilon)}{(\Delta_\perp^2)^{-2\epsilon}} \left(\left[-\frac{2}{3\epsilon} + 2 - \frac{1}{3(1 + \epsilon)} \right] \right. \\
 &\times 2 \text{Tr}\{t^a \partial_i U_x t^b \partial_i U_x^\dagger\} - \frac{4\epsilon}{3(1 + \epsilon)} \frac{\Delta_i \Delta_j}{\Delta_\perp^2} \\
 &\left. \times 2 \text{Tr}\{t^a \partial_i U_x t^b \partial_j U_x^\dagger\} \right), \quad (\text{A24})
 \end{aligned}$$

so we obtain

$$\begin{aligned}
 \text{Tr}\{\partial_i^x U_x \partial_i^y U_y^\dagger\} \xrightarrow{x_\perp \rightarrow y_\perp} &\frac{\alpha_s^2 n_f}{\pi^2} \Delta \eta \frac{B(2 - \epsilon, 2 - \epsilon)}{\epsilon} \frac{\Gamma(-2\epsilon)}{(\Delta_\perp^2)^{-2\epsilon}} \\
 &\times U_x^{ab} \partial_\perp^2 U_x^{ab} + \frac{\alpha_s^2 n_f}{4\pi^2 N_c} \Delta \eta B(1 - \epsilon, 1 - \epsilon) \\
 &\times \frac{\Gamma(-2\epsilon)}{(\Delta_\perp^2)^{-2\epsilon}} \left[\left[\frac{2}{3\epsilon} - 2 + \frac{1}{3(1 + \epsilon)} \right] \delta_{ij} \right. \\
 &\left. + \frac{4\epsilon}{3(1 + \epsilon)} \frac{\Delta_i \Delta_j}{\Delta_\perp^2} \right] \text{Tr}\{\partial_i U_x \partial_j U_x^\dagger\}. \quad (\text{A25})
 \end{aligned}$$

Last, we need to write down the sum of $1/\epsilon$ counterterms to diagrams in Fig. 11(a)–11(g). It can be read from the first term in the r.h.s. of Eq. (A16):

$$-\frac{\alpha_s^2 n_f}{12\pi^2 \epsilon} \Delta \eta \frac{\Gamma(-2\epsilon)}{(\Delta_\perp^2)^{-2\epsilon}} U_x^{ab} \partial_\perp^2 U_x^{ab}. \quad (\text{A26})$$

Adding the counterterm (A26) to Eq. (A25) we get

$$\begin{aligned}
 \text{Tr}\{\partial_i^x U_x \partial_i^y U_y^\dagger\} \xrightarrow{x_\perp \rightarrow y_\perp} &\frac{\alpha_s^2 n_f}{\pi^2} \Delta \eta \left[\frac{B(2 - \epsilon, 2 - \epsilon)}{\epsilon} \frac{\Gamma(-2\epsilon)}{(\Delta_\perp^2)^{-2\epsilon}} \right. \\
 &- \frac{1}{12\epsilon} \frac{\Gamma(-2\epsilon)}{(\Delta_\perp^2)^{-2\epsilon}} \left. \right] U_x^{ab} \partial_\perp^2 U_x^{ab} \\
 &+ \frac{\alpha_s^2 n_f}{4\pi^2 N_c} \Delta \eta B(1 - \epsilon, 1 - \epsilon) \\
 &\times \frac{\Gamma(-2\epsilon)}{(\Delta_\perp^2)^{-2\epsilon}} \left[\left(\frac{2}{3\epsilon} - 2 + \frac{1}{3(1 + \epsilon)} \right) \delta_{ij} \right. \\
 &\left. + \frac{4\epsilon}{3(1 + \epsilon)} \frac{\Delta_i \Delta_j}{\Delta_\perp^2} \right] \text{Tr}\{\partial_i U_x \partial_j U_x^\dagger\}, \quad (\text{A27})
 \end{aligned}$$

which coincides with Eq. (22).

APPENDIX B: COMPARISON WITH THE TRIUMVIRATE OF COUPLING CONSTANTS

It is instructive to compare our result to the recent paper [16] where the NLO BK equation is rewritten in terms of three effective coupling constants.

In the momentum space, there are three coupling constants as seen from the bubble-chain picture, see Eq. (46). Unfortunately, the Fourier transformation to the coordinate space can be performed explicitly only for a couple of first terms of the expansion $\alpha_s(p^2) \simeq \alpha_s - \frac{b\alpha_s}{4\pi} \ln p^2/\mu^2 + (\frac{b\alpha_s}{4\pi} \ln p^2/\mu^2)^2$. The result of the corresponding Fourier transformation is given by the sum of Eqs. (40) and (51):

$$\begin{aligned}
 \frac{d}{d\eta} \text{Tr}\{U_x U_y^\dagger\} &= \frac{\alpha_s}{2\pi^2} \int d^2 z [\text{Tr}\{U_x U_z^\dagger\} \text{Tr}\{U_z U_y^\dagger\} - N_c \text{Tr}\{U_x U_y^\dagger\}] \left[\frac{(x-y)^2}{X^2 Y^2} \left[1 + \frac{b\alpha_s}{4\pi} \left(\ln(x-y)^2 \mu^2 + \frac{5}{3} \right) \right. \right. \\
 &+ \left. \left. \left(\frac{b\alpha_s}{4\pi} \right)^2 \ln^2(x-y)^2 \mu^2 \right] + \frac{b\alpha_s}{4\pi} \frac{1}{X^2} \ln \frac{X^2}{Y^2} \left[1 + \frac{b\alpha_s}{4\pi} \ln(x-y)^2 \mu^2 + \frac{b\alpha_s}{4\pi} \ln X^2 \mu^2 \right] \right] \\
 &- \frac{b\alpha_s}{4\pi} \frac{1}{Y^2} \ln \frac{X^2}{Y^2} \left[1 + \frac{b\alpha_s}{4\pi} \ln(x-y)^2 \mu^2 + \frac{b\alpha_s}{4\pi} \ln Y^2 \mu^2 \right] + \frac{\alpha_s^2}{\pi^4} n_f \text{Tr}\{t^a U_x t^b U_y^\dagger\} \\
 &\times \int \frac{d^2 z' d^2 z''}{(z-z')^4} \text{Tr}\{t^a U_z t^b U_{z'}^\dagger - t^a U_z t^b U_{z''}^\dagger\} \left[1 - \frac{X'^2 Y^2 + Y'^2 X^2 - (x-y)^2 (z-z')^2}{2(X'^2 Y^2 - Y'^2 X^2)} \ln \frac{X'^2 Y^2}{Y'^2 X^2} \right] \quad (\text{B1})
 \end{aligned}$$

This result coincides with the calculation of Kovchegov and Weigert, but the interpretation is different. I extrapolate the $\ln + \ln^2$ terms in the above equation as follows:

$$\begin{aligned}
\frac{d}{d\eta} \text{Tr}\{U_x U_y^\dagger\} &= \frac{\alpha_s((x-y)^2 e^{5/3})}{2\pi^2} \int d^2 z [\text{Tr}\{U_x U_z^\dagger\} \text{Tr}\{U_z U_y^\dagger\} - N_c \text{Tr}\{U_x U_y^\dagger\}] \left[\frac{(x-y)^2}{X^2 Y^2} + \frac{1}{X^2} \left(\frac{\alpha_s(X^2)}{\alpha_s(Y^2)} - 1 \right) \right. \\
&\quad \left. + \frac{1}{Y^2} \left(\frac{\alpha_s(Y^2)}{\alpha_s(X^2)} - 1 \right) \right] + \frac{\alpha_s^2}{\pi^4} n_f \text{Tr}\{t^a U_x t^b U_y^\dagger\} \int \frac{d^2 z d^2 z'}{(z-z')^4} \text{Tr}\{t^a U_z t^b U_{z'}^\dagger - t^a U_z t^b U_{z'}^\dagger\} \\
&\quad \times \left\{ 1 - \frac{X'^2 Y^2 + Y'^2 X^2 - (x-y)^2 (z-z')^2}{2(X'^2 Y^2 - Y'^2 X^2)} \ln \frac{X'^2 Y^2}{Y'^2 X^2} \right\}, \tag{B2}
\end{aligned}$$

and interpret it as the $\alpha_s(e^{5/3}|x-y|^2)$ times BK kernel plus two $O(\alpha_s^2)$ corrections with different functional form of the kernel and a more complicated argument of coupling constant (in the case of the last term, I have not calculated that argument even in the leading order). The authors of Ref. [16] extrapolate Eq. (B1) in a different way

$$\begin{aligned}
\frac{d}{d\eta} \text{Tr}\{U_x U_y^\dagger\} &= \frac{1}{2\pi^2} \int d^2 z [\text{Tr}\{U_x U_z^\dagger\} \text{Tr}\{U_z U_y^\dagger\} - N_c \text{Tr}\{U_x U_y^\dagger\}] \left[\frac{1}{X^2} \alpha_s(X^2 e^{5/3}) + \frac{1}{Y^2} \alpha_s(Y^2 e^{5/3}) \right. \\
&\quad \left. - \frac{2(x-z, y-z)}{X^2 Y^2} \frac{\alpha_s(X^2 e^{5/3}) \alpha_s(Y^2 e^{5/3})}{\alpha_s(R^2)} \right] + \frac{\alpha_s^2}{\pi^4} n_f \text{Tr}\{t^a U_x t^b U_y^\dagger\} \int \frac{d^2 z d^2 z'}{(z-z')^4} \text{Tr}\{t^a U_z t^b U_{z'}^\dagger - t^a U_z t^b U_{z'}^\dagger\} \\
&\quad \times \left\{ 1 - \frac{X'^2 Y^2 + Y'^2 X^2 - (x-y)^2 (z-z')^2}{2(X'^2 Y^2 - Y'^2 X^2)} \ln \frac{X'^2 Y^2}{Y'^2 X^2} \right\}, \tag{B3}
\end{aligned}$$

where R^2 is some scale interpolating between X^2 and Y^2 (the explicit form can be found in Ref. [16]). Theoretically, until the Fourier transformations in all orders in $\ln p^2/\mu^2$ are performed, both of these interpretations are models of the high-order behavior of running coupling constant. I have a more simple model plus two corrections and Ref. [16] has a more complicated model plus only one correction. The convenience of these models can be checked by the numerical estimates of the size of the neglected term(s) in comparison to terms taken into account by the model.

-
- [1] I. Balitsky, in *High-Energy QCD and Wilson Lines*, edited by M. Shifman, At the frontier of particle physics, Vol. 2 (World Scientific, Singapore, 2001), p. 1237–1342.
- [2] A. H. Mueller, Nucl. Phys. **B415**, 373 (1994); A. H. Mueller and Bimal Patel, Nucl. Phys. **B425**, 471 (1994).
- [3] N. N. Nikolaev and B. G. Zakharov, Phys. Lett. B **332**, 184 (1994); Z. Phys. C **64**, 631 (1994); N. N. Nikolaev, B. G. Zakharov, and V. R. Zoller, JETP Lett. **59**, 6 (1994).
- [4] V. S. Fadin, E. A. Kuraev, and L. N. Lipatov, Phys. Lett. B **60**, 50 (1975); I. I. Balitsky and L. N. Lipatov, Sov. J. Nucl. Phys. **28**, 822 (1978).
- [5] L. V. Gribov, E. M. Levin, and M. G. Ryskin, Phys. Rep. **100**, 1 (1983); A. H. Mueller and J. W. Qiu, Nucl. Phys. **B268**, 427 (1986); A. H. Mueller, Nucl. Phys. **B335**, 115 (1990).
- [6] L. McLerran and R. Venugopalan, Phys. Rev. D **49**, 2233 (1994); **49**, 3352 (1994).
- [7] J. Jalilian-Marian, A. Kovner, A. Leonidov, and H. Weigert, Nucl. Phys. **B504**, 415 (1997); Phys. Rev. D **59**, 014014 (1998); J. Jalilian-Marian, A. Kovner, and H. Weigert, Phys. Rev. D **59**, 014015 (1998); A. Kovner, J. G. Milhano, and H. Weigert, Phys. Rev. D **62**, 114005 (2000); E. Iancu, A. Leonidov, and L. McLerran, Nucl. Phys. **A692**, 583 (2001); Phys. Lett. B **510**, 133 (2001); E. Ferreiro, E. Iancu, A. Leonidov, and L. McLerran, Nucl. Phys. **A703**, 489 (2002).
- [8] Yu. V. Kovchegov, Phys. Rev. D **60**, 034008 (1999); **61**, 074018 (2000).
- [9] I. Balitsky, Nucl. Phys. **B463**, 99 (1996).
- [10] J. L. Albacete, N. Armesto, J. G. Milhano, C. A. Salgado, and U. A. Wiedemann, Phys. Rev. D **71**, 014003 (2005).
- [11] V. S. Fadin and R. Fiore, Phys. Rev. D **72**, 014018 (2005).
- [12] I. Balitsky and A. V. Belitsky, Nucl. Phys. **B629**, 290 (2002).
- [13] M. Beneke, Phys. Rep. **317**, 1 (1999); M. Beneke and V. M. Braun, *Renormalons and Power Corrections*, edited by M. Shifman, At the Frontier of Particle Physics, Vol. 3 (World Scientific, Singapore, 2001) p. 1719–1773.
- [14] S. J. Brodsky, G. P. Lepage, and P. B. Mackenzie, Phys. Rev. D **28**, 228 (1983).
- [15] M. Beneke and V. M. Braun, Phys. Lett. B **348**, 513 (1995).
- [16] Yu. Kovchegov and H. Weigert, hep-ph/0609090.
- [17] I. Balitsky, Phys. Rev. D **60**, 014020 (1999).
- [18] V. S. Fadin, R. Fiore, and A. Papa, Phys. Rev. D **60**, 074025 (1999).
- [19] V. S. Fadin and L. N. Lipatov, Phys. Lett. B **429**, 127 (1998); G. Camici and M. Ciafaloni, Phys. Lett. B **430**, 349 (1998).
- [20] E. Levin, Nucl. Phys. **B453**, 303 (1995).
- [21] In principle, it should be supported by the (numerical) analysis of third (and higher) higher orders in $\ln p^2/\mu^2$, see the discussion in the Appendix B.
- [22] Y. Hatta, E. Iancu, L. McLerran, A. Stasto, and D. N. Triantafyllopoulos, Nucl. Phys. **A764**, 423 (2006); I. Balitsky, Phys. Rev. D **72**, 074027 (2005).

- [23] I. I. Balitsky, Phys. Lett. B **124**, 230 (1983).
- [24] I. Balitsky and V.M. Braun, Nucl. Phys. **B311**, 541 (1989); **B361**, 93 (1991).
- [25] The terms proportional to γ_5 may cause problems in the dimensional regularization so one needs to return to the previous expression for the quark propagator with three antisymmetrized γ -matrices. However, for the particular contributions which we are interested in the product of two quark propagators at $d_{\perp} \neq 2$ is the same as the product of two expressions (A5).
- [26] Up to a possible pure gauge field which does not change the result of the analysis, see the discussion in Ref. [1]).